A DETERMINATION OF THE SULFUR ISOTOPIC SIGNATURE OF AN ORE-FORMING FLUID FROM THE SIERRITA PORPHYRY COPPER DEPOSIT PIMA COUNTY, ARIZONA

by

Kent Turner, Jr.

A Thesis Submitted to the Faculty of the

DEPARTMENT OF GEOSCIENCES

In partial Fulfillment of the Requirements
For the Degree of

MASTER OF SCIENCE

In the Graduate College

The University of Arizona

1 9 8 3

STATEMENT BY AUTHOR

This thesis has been submitted in partial fulfillment of requirements for an advanced degree at the University of Arizona and is deposited in the University Library to be made available to borrowers under rules of the Library.

Brief quotations from this thesis are allowable without special permission, provided that accurate acknowledgment of source is made. Requests for permission for extended quotation from or reproduction of this manuscript in whole or in part may be granted by the head of the major department or the Dean of the Graduate College when in his judgment the proposed use of the material is in the interests of scholarship. In all other instances, however, permission must be obtained from the author.

SIGNED: _____

APPROVAL BY THESIS DIRECTOR

This thesis has been approved on the date shown below:

Richard E. Beane — 17 May, 1983

Professor of Geosciences — Date

TABLE OF CONTENTS

LIST OF ILLUSTRATIONS

LIST OF TABLES

ABSTRACT

The application of sulfur isotopy to studies on the genesis of porphyry copper deposits requires knowledge of the physio-chemical parameters governing aqueous sulfur distribution accompanied by the isotopic composition of precipitated sulfur-bearing minerals. Detailed study of a single vein from the Sierrita deposit permitted the determination of the parameters: temperature (350°C), pressure (330 bars), salinity (1.14 molal), f_{O_2} ($10^{-27.5}$), pH (5.8) and sodium, potassium and calcium activities (6.3×10^{-2}, 9.8×10^{-3} , 1.0×10^{-5}, respectively) from which the relative molar distribution of aqueous sulfur was calculated to be 50% sulfide and 50% sulfate. Isotopic analyses of vein sulfides (pyrite = -0.8°/oo, chalcopyrite = -2.0°/oo) and sulfates (anhydrite = +8.8°/oo) indicate a system which is not in isotopic equilibrium. This lack of equilibrium precludes quantitative calculation of the isotopic composition of aqueous sulfur. The concept of systematic disequilibrium may allow interpretation of these results that imply either an igneous or a dual igneous - sedimentary sulfate sulfur source.

INTRODUCTION AND BACKGROUND

Introduction

The source of the ore-forming materials, and the relative importance of 'magmatic' vs 'meteoric' waters in the derivation and distribution of these materials are of continuing controversy in the study of the origins and genesis of porphyry copper deposits. To date, no satisfactory method of directly characterizing or tracing the source of the metals has been found. However, porphyry copper deposits are more than simply economic accumulations of copper and molybdenum, they are also significant sulfur anomalies. Sulfur locally composes up to 6% of mineralized rock (Chaffee, 1982), which corresponds to a 200- to 1000-fold increase above concentrations in equivalent non-mineralized rocks (Banks, 1982; Turekian, 1972). It is the purpose of this study to isotopically characterize the sulfur in the hydrothermal fluid from which the mineralization formed, for the purpose of defining a possible source, or sources, of sulfur in a typical porphyry copper deposit.

Early applications of sulfur isotope studies to hydrothermal ore deposits and, in particular, attempts to identify possible source(s) of the introduced sulfur, consisted primarily of determining the sulfur isotopic composition of sulfur-bearing minerals and comparing the results with 'typical' sulfur isotopic compositions from various possible sulfur sources. However, if the source of the sulfur

is to be accurately identified, it is not sufficient simply to analyze the minerals which are present in the system today. Rather, it is necessary to determine the isotopic composition of the sulfur in the mineralizing solution which may be significantly different from that of related sulfur-bearing minerals.

Samples from the Duval Corporation's Sierrita porphyry copper deposit, located 15 miles south of Tucson in Pima County, Arizona (Fig. 1), were chosen for this study because extensive previous work (West and Aiken, 1980; Preece and Beane, 1982; Aiken and West, 1978) has defined mineral assemblages which can be employed to determine the variables which control distribution and isotopic composition of sulfur in the hydrothermal fluid. Sierrita also offers the simplification of having been only weakly modified by supergene processes. The vein and wall rock minerals in the deeper exposures of mineralization are texturally and, by implication, chemically relatively unaffected by post mineralization events (West and Aiken, 1980; Preece and Beane, 1982; Aiken and West, 1978). Samples for this study were collected from several locations within the Sierrita pit where favorable mineral assemblages were present. Petrographic, fluid inclusion, scanning electron microprobe and sulfur isotope analyses were conducted in order to evaluate the parameters required to calculate the sulfur isotopic composition of the hydrothermal fluid.

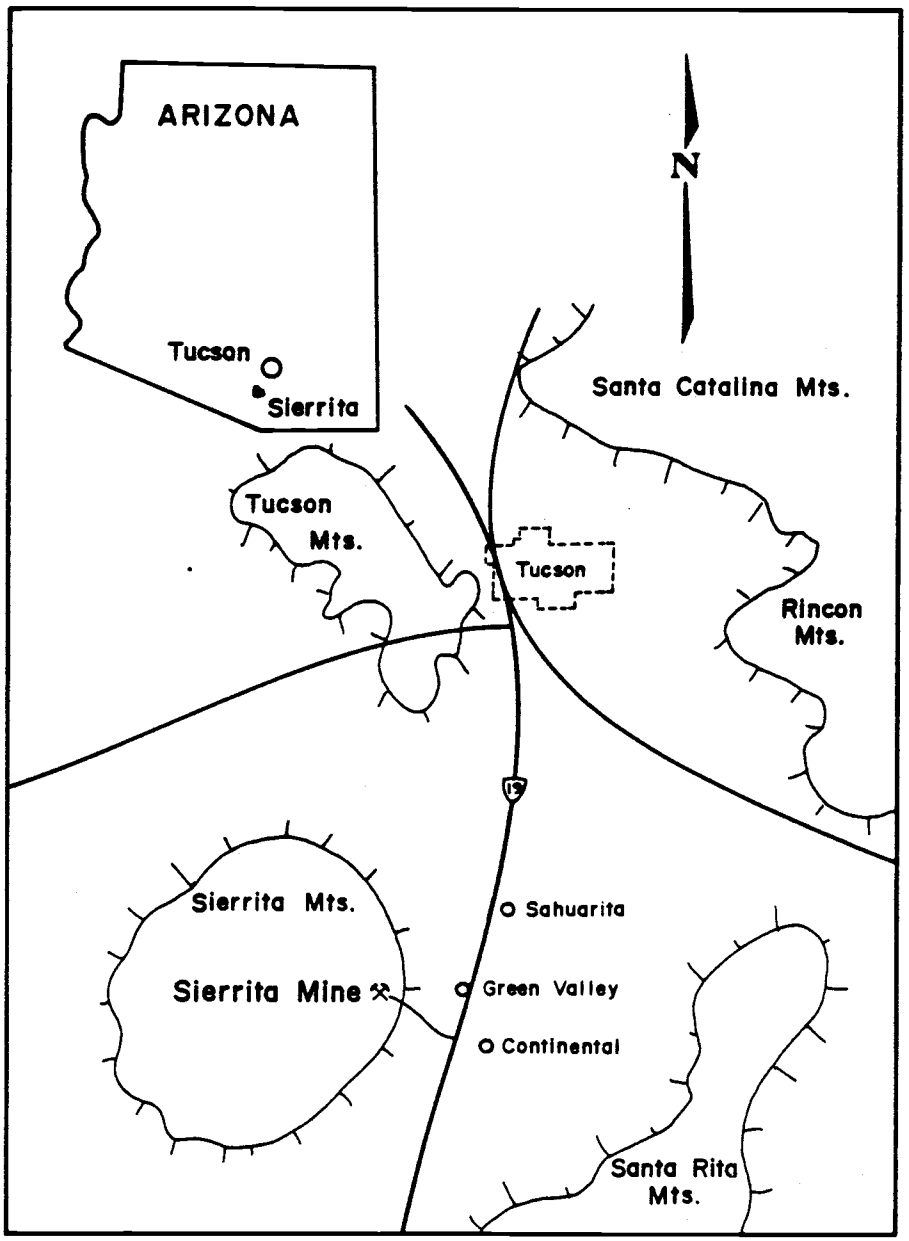

Figure 1. Location of the Sierrita porphyry copper deposit.

Theory of Sulfur Isotopy in Hydrothermal Environments

The theory of the application of sulfur isotopy to hydrothermal systems will be briefly reviewed below. For more extensive treatments of the subject, the reader is referred to Ohmoto and Rye (1979), Faure (1977), Rye and Ohmoto (1974), Ohomoto (1972) and Sakai (1968).

There are four stable isotopes of sulfur in nature; ^{32}S, ^{33}S, ^{34}S and ^{36}S having approximate relative distributions of 95%, 0.75%, 4.2% and 0.002%, respectively (Ohmoto and Rye, 1979). Most sulfur isotope studies have been made on variations in the ratio of the two most abundant isotopes, ^{34}S and ^{32}S. The isotopic composition of a given sulfur-bearing species is usually given as a $\delta^{34}S$ value, where $\delta^{34}S$ is the per mil variation in the molar $^{34}S/^{32}S$ ratio of the sample with respect to the molar $^{34}S/^{32}S$ ratio of a standard as defined by:

$$\delta^{34}S_{sample} = \left[\frac{(^{34}S / ^{32}S)_{sample}}{(^{34}S / ^{32}S)_{standard}} - 1 \right] \times 1000 \qquad (1)$$

The generally accepted standard for sulfur isotopy is the ^{34}S to ^{32}S ratio of troilite from the Canon Diablo meteorite, in which $^{34}S/^{32}S$ = 0.0450045 (Ault and Jensen, 1963).

The variation in sulfur isotopic composition between two species 'a' and 'b' is expressed by the relative isotopic enrichment factor, Δ_{a-b}, where:

$$\Delta_{a-b} = \delta^{34}S_a - \delta^{34}S_b \quad (2)$$

Under equilibrium conditions Δ_{a-b} is approximated using the isotopic fractionation factor α_{a-b}:

$$\Delta_{a-b} \approx 1000 \ln\alpha_{a-b} \quad (3)$$

From experimental and theoretical data α_{a-b} has been found to be a function solely of temperature at pressures less than 10 kb (Ohmoto and Rye, 1979). This relationship is expressed by:

$$1000 \ln\alpha_{a-b} = (A/T^2) \times 10^6 + (B/T) \times 10^3 + C \quad (4)$$

where A, B and C are coefficients characteristic of the species pair a-b (Ohmoto and Rye, 1979).

Fluid inclusion studies have demonstrated that the ore-forming fluids of porphyry copper systems are essentially alkali - chloride aqueous solutions (Nash, 1975; Denis, 1974; Roedder, 1972). At temperatures below 500°C and under geologically reasonable conditions, the important sulfur-bearing species in an alkali - chloride solution are: H_2S°, HS^-, S^{2-}, SO_4^{2-}, HSO_4^-, $NaSO_4^-$, KSO_4^- and $CaSO_4^\circ$ (Ohmoto,

1972). The sulfur isotopic composition of a hydrothermal solution whose sulfur is distributed among these species is equal to the average of the $\delta^{34}S$ value of each species, weighted by the relative proportion of total sulfur composing that species. This relationship is summarized by:

$$\delta^{34}S_{\Sigma S_{aq}} = \sum_i (\delta^{34}S_i \cdot X_i) \tag{5}$$

where X_i is:

$$X_i = m_i / m_{\Sigma S_{aq}} \tag{6}$$

and:

$$m_{\Sigma S_{aq}} = m_{H_2S^o} + m_{HS^-} + m_{S^{2-}} + m_{SO_4^{2-}} + m_{HSO_4^-} + m_{NaSO_4^-} + m_{KSO_4^-} + m_{CaSO_4^o} \tag{7}$$

Determination of the total isotopic composition of dissolved sulfur (Equation 5) can be made in two ways. In one case, the isotopic composition and molality of each of the individual sulfur-

bearing aqueous species is directly determined. Alternatively, at chemical equilibrium, the isotopic composition of a single species is determined, and then with knowledge of the physical and chemical parameters influencing chemical speciation and isotope partitioning, the isotopic compositions and relative concentrations of the other aqueous sulfur-bearing species are calculated. Direct measurements of the concentration and sulfur isotopic composition of aqueous sulfur-bearing species in the mineralizing fluids of porphyry copper deposits are rarely possible, because these fluids are no longer present in such systems today except in fluid inclusions whose small size introduces practical sampling difficulties. Therefore, it is generally necessary to calculate the sulfur isotopic composition of the fluid from the calculated distribution and isotopic compositions of aqueous sulfur species which requires knowledge of certain physical and chemical parameters, in addition to sulfur isotope data derived from minerals.

As stated above, isotope partitioning among the various sulfur-bearing species, under the conditions of porphyry copper formation, is a function solely of temperature. The absolute $\delta^{34}S$ value for each species can be calculated from the measured $\delta^{34}S$ value of a sulfur-bearing mineral precipitated from the solution if the temperature of that the solution at the time of precipitation is known. The relative distribution of the aqueous sulfur species of interest (H_2S°, HS^-, S^{2-}, SO_4^{2-}, HSO_4^-, $NaSO_4^-$, KSO_4^- and $CaSO_4^\circ$) can be calculated using the following equilibrium relations:

$$H_2S^\circ = HS^- + H^+ \quad (8)$$

$$H_2S^\circ = S^{2-} + 2\ H^+ \quad (9)$$

$$H_2S^\circ + 2\ O_2 = SO_4^{2-} + 2\ H^+ \quad (10)$$

$$H_2S^\circ + 2\ O_2 = HSO_4^- + H^+ \quad (11)$$

$$H_2S^\circ + 2\ O_2 + Na^+ = NaSO_4^- + 2\ H^+ \quad (12)$$

$$H_2S^\circ + 2\ O_2 + K^+ = KSO_4^- + 2\ H^+ \quad (13)$$

$$H_2S^\circ + 2\ O_2 + Ca^{2+} = CaSO_4^\circ + 2\ H^+ \quad (14)$$

Employing the equilibrium reaction constant, K, for each of these reactions yields the following equations:

$$K_8 = \frac{(a_{HS^-})\ (a_{H^+})}{(a_{H_2S^o})} \quad (15)$$

$$K_9 = \frac{(a_{S^{2-}})\ (a_{H^+})^2}{(a_{H_2S^o})} \quad (16)$$

$$K_{10} = \frac{(a_{SO_4^{2-}})\ \ (a_{H^+})^2}{(a_{H_2S^o})\ (f_{o_2})^2} \quad (17)$$

$$K_{11} = \frac{(a_{HSO_4^-})\ (a_{H^+})}{(a_{H_2S^o})\ (f_{O_2})^2} \tag{18}$$

$$K_{12} = \frac{(a_{NaSO_4})\ (a_{H^+})^2}{(a_{H_2S^o})\ (f_{O_2})^2\ (a_{Na^+})} \tag{19}$$

$$K_{13} = \frac{(a_{KSO_4^-})\ (a_{H^+})^2}{(a_{H_2S^o})\ (f_{O_2})^2\ (a_{K^+})} \tag{20}$$

$$K_{14} = \frac{(a_{CaSO_4^o})\ (a_{H^+})^2}{(a_{H_2S^o})\ (f_{O_2})^2\ (a_{Ca^{2+}})} \tag{21}$$

The molality of these species, m, can be introduced by employing the activity coefficient, γ, for each species from the relationship:

$$a_i = m_i \cdot \gamma_i \tag{22}$$

Rearranging Equations 15-21 and using the activity - molality relationship in Equation 22 yields the following set of reactions which define the relative molalities of the aqueous sulfur species:

$$m_{HS^-} = \frac{(K_8)\ (m_{H_2S^o})\ (\gamma_{H_2S^o})}{(\gamma_{HS^-})\ (a_{H^+})} \tag{23}$$

$$m_{S^{2-}} = \frac{(K_9)\ (m_{H_2S^o})\ (\gamma_{H_2S^o})}{(\gamma_{S^{2-}})\ (a_{H^+})^2} \tag{24}$$

$$m_{SO_4^{2-}} = \frac{(K_{10})\ (m_{H_2S^o})\ (\gamma_{H_2S^o})\ (f_{O_2})^2}{(\gamma_{SO_4^{2-}})\ (a_{H^+})^2} \tag{25}$$

$$m_{HSO_4^-} = \frac{(K_{11})\ (m_{H_2S^o})\ (\gamma_{H_2S^o})\ (f_{O_2})^2}{(\gamma_{HSO_4^-})\ (a_{H^+})} \tag{26}$$

$$m_{NaSO_4^-} = \frac{(K_{12})(m_{H_2S^o})(\gamma_{H_2S^o})(f_{O_2})^2(a_{Na^+})}{(\gamma_{NaSO_4^-})\ (a_{H^+})^2} \tag{27}$$

$$m_{KSO_4^-} = \frac{(K_{13})\ (m_{H_2S^o})\ (\gamma_{H_2S^o})\ (f_{O_2})^2\ (a_{K^+})}{(\gamma_{KSO_4^-})\ (a_{H^+})^2} \tag{28}$$

$$m_{CaSO_4^o} = \frac{(K_{14})\ (m_{H_2S^o})\ (\gamma_{H_2S^o})\ (f_{O_2})^2\ (a_{Ca^{2+}})}{(\gamma_{CaSO_4^o})\ (a_{H^+})^2} \tag{29}$$

By solving Equations 23-29, the mole fractions of the various sulfur-bearing species can be determined, and if the absolute molality of H_2S°, or any of the other sulfur-bearing species, is determined, then the absolute molality of each can be calculated.

The equilibrium reaction constant, K, for any given reaction is a function of temperature and pressure (Garrels and Christ, 1965). The activity coefficient, γ, for any given species is a function of temperature, pressure and ionic strength of the solution (Garrels and Christ, 1965). Thus, in order to calculate the relative distribution of aqueous sulfur species from Equations 23-29, it is necessary to establish, or approximate; temperature, pressure, ionic strength, oxygen fugacity, pH and activities of Na^+, K^+ and Ca^{2+} in the hydrothermal solution.

Temperature, ionic strength (salinity) and, less readily, pressure can be determined from analysis of fluid inclusions in hydrothermal minerals. Oxygen fugacity, pH and the activities of Na^+, K^+ and Ca^{2+} may, under proper conditions, be calculated using equilibrium relations among minerals formed in the rock by the mineralizing solution.

Geology of the Sierrita Deposit

The Sierrita porphyry copper deposit, together with the Esperanza deposit, is part of the Sierrita - Esperanza porphyry copper complex located at the southeastern end of the Sierrita Mountains (Fig. 1). Detailed descriptions of the geology, structure and mineralization of the system are given by West and Aiken (1982), Aiken and West (1978), Smith (1975) and Lynch (1966). Only a brief description of the general geology within the Sierrita pit will be included here.

Within the pit at Sierrita three intrusive units dominate the geology: the Jurassic - Triassic Harris Ranch quartz monzonite, the 67 m.y. (Cooper, 1973) biotite quartz diorite and the 57 m.y. (Cooper, 1973) Ruby Star quartz monzonite porphyry (Fig. 2). Average modal mineralogies of these three intrusives, as they are found in the mine, are listed in Table 1. The Ruby Star quartz monzonite porphyry is a facies of the batholithic Ruby Star granodiorite which makes up the bulk of the Sierrita Mountains. This porphyritic differentiate is spatially and structurally at the center of the Sierrita - Esperanza porphyry copper system (Thompson, 1981; Haynes, 1980) and is thought to be responsible for the mineralization (West and Aiken, 1982; Aiken and West, 1978; Smith, 1975).

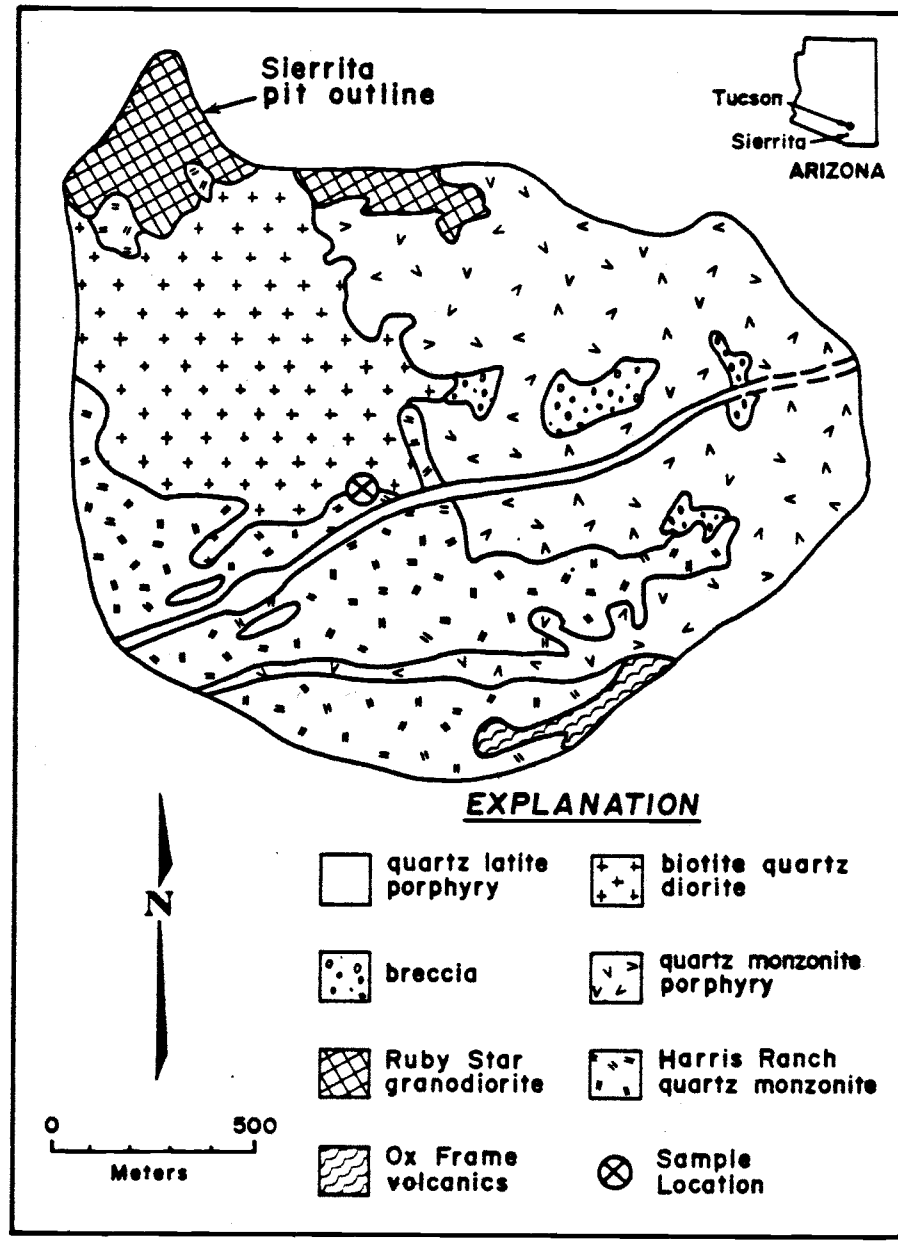

Figure 2. General geology of the Sierrita open pit. After Preece 1978.

Table 1. Average mineralogic compositions of the three main intrusive units in the Sierrita open pit (from West and Aiken, 1982).

	Harris Ranch Quartz Monzonite	Biotite Quartz Diorite	Ruby Star Quartz Monzonite Porphyry
Quartz	25	7	25
Potassium Feldspar	35	7	25
Plagioclase	25	30	35
Biotite	5	25	5
Hornblende	-	25	-
Accessory Minerals	epidote tourmaline chlorite sericite pyrite	actinolite magnetite epidote chlorite pyrite	chlorite apatite zircon epidote magnetite

ANALYTICAL METHODS

Sample Descriptions

Several hand samples were collected from inside the Sierrita pit near the contact between the biotite quartz diorite and the Harris Ranch quartz monzonite within 250 m of the Ruby Star quartz monzonite porphyry intrusive contact (Fig. 2). After hand lens examination of slabbed surfaces of these samples, a single vein from the biotite quartz diorite was chosen for study. The selection was based on the presence of wall rock alteration and vein-filling mineralogies which would provide a means of establishing the composition of the hydrothermal solution from which the vein formed. The portion of the vein studied was spacially isolated from other veins (2-3 cm minimum) so that vein selvage alteration could be unequivocally ascribed to this solution conduit.

The original modal mineralogy of the biotite quartz diorite sample chosen for study was: plagioclase feldspar 50%, biotite 25%, hornblende 20%, and quartz 5% with minor magnetite. This mineralogy was determined by petrographic microscope examination of a polished thin section from the least altered wall rock in the sample. Vein controlled alteration consisted of: partial to complete destruction of hornblende, commonly by conversion to biotite; chloritization of both 'alteration' and 'original' biotites; and weak to moderate dusting of

sericite in feldspars and, to a lesser extent, chlorites. Each of these alteration manifestations was seen to be strongest near the vein edge, diminishing to nearly absent over a very short distance into the wall rock (generally less than 1 cm).

The vein contains quartz, epidote, pyrite, chalcopyrite and anhydrite with trace amounts of molybdenite and magnetite. The contact between vein minerals and wall rock is sharp along most of its length in the sample. It is marked by a sudden change from relatively fine grained (less than 0.5 mm) quartz, sericite-dusted feldspar and chlorite in the wall rock to relatively coarse (greater than 1 mm in diameter) vein quartz. Very fine molybdenite flakes (less than 0.1 mm in length) are present along the vein margin and are oriented perpendicular to the vein wall. The central portion of the vein contains a more complex mineral assemblage consisting of quartz, which is optically identical to that along the vein edge, epidote, pyrite, chalcopyrite and anhydrite. Trace amounts of magnetite occur as tiny blebs in pyrite grains. The vein-filling mineralogy and wall rock alteration assemblage are summarized in Table 2. It is not possible to say that all vein-filling minerals observed were coprecipitated in euqilibrium with one another. However, each mineral, with the exception of magnetite, is in contact with every other vein-filling mineral at some point along the studied section of the vein. This distribution of mineral grains in the vein is such that a solution depositing any one mineral would be in intimate physical contact with any previously deposited minerals, and since no evidence was seen to

Table 2. Summary of original wall rock mineralogy, vein-filling mineralogy, and wall rock alteration adjacent to the vein as determined by petrographic examination.

Original Wall Rock Mineralogy of Studied Sample:

Plagioclase	50%
Biotite	25
Hornblende	20
Quartz	5
Magnetite	tr

Mineralogy of Vein Studied:

Edge;

Quartz
Molybdenite

Center;

Quartz	Pyrite
Epidote	Chalcopyrite
Anhydrite	Magnetite

Wall Rock Alteration Adjacent to Vein Studied:

Hornblende ⟶ Biotite ⟶ Chlorite

Biotite ⟶ Chlorite

Plagioclase ⟶ weak Sericitization

indicate either dissolution or alteration of these minerals it is unlikely that any one mineral is seriously out of equilibrium with any others present.

The sharp contact between the wall rock and vein quartz along the vein edge is transected at irregular intervals by vein-filling epidote (and to a much lesser extent anhydrite), which embays the wall rock. This epidote is generally finer grained than epidote at the center of the vein. Small quartz grains are also present in these embayments and are thought to be surviving wall rock quartz. The epidote embayments are rimmed by a thin (less than 0.5 mm thick) selvage dominated by chlorite which in turn gives way to the typical vein-edge wall rock assemblage described above.

These embayments, along with the observed weakening of alteration manifestations with distance away from the vein indicate that the hydrothermal fluid was in chemical contact with the minerals present in the wall rock. While it can not be unequivocally demonstrated that the alteration mineral assemblage immediately adjacent to the vein was in equilibrium with the mineralizing solution, the alteration minerals almost certainly formed by reaction with the solution. It is an assumption of this study that chemical equilibrium between the mineralizing solution and the wall rock alteration assemblage was closely approached.

Vein and wall rock alteration mineral assemblages comparable to those seen in the sample selected for this study are commonly reported from the biotite quartz diorite (Preece and Beane, 1982;

Smith, 1975). From cross-cutting relationships in a single hand sample, Preece and Beane (1982) documented a minimum of five cycles of development of similar alteration assemblages in the biotite quartz diorite. Mineral compositions of these veins, along with the vein described in this study, are listed in Table 3. Each cycle begins with an early vein-edge assemblage of quartz, biotite and feldspar (both potassic and sodic) which is followed by an assemblage of quartz, epidote, chlorite, pyrite and chalcopyrite with minor magnetite and molybdenite. The vein selected for this study contains a mineral assemblage which corresponds with that of the later portion of one of Preece and Beane's (1982) cycles and lacks the biotite and feldspar characteristic of the early part of each cycle. From this observation, it is inferred that the portion of the vein studied was closed to fluid circulation during the early 'potassic' stage defined by Preece and Beane, and was opened when circulating fluids were depositing the later 'propylitic' assemblage.

Fluid Inclusion Analyses

Fluid inclusion analysis of vein-filling quartz was carried out using standard fluid inclusion heating-freezing techniques. Doubly polished (0.3 micron grit) sections 100-200 microns thick were prepared. The analyses were conducted on an S.G.E. Inc., Model III dual purpose gas flow heating/freezing stage at the University of Arizona and at AMAX Exploration Inc. of Tucson, Arizona. Heating was accomplished by passing air over an electric torch and then over the

Table 3. Mineralogy and fluid inclusion data determined by Preece and Beane (1982) for a set of veins from the biotite quartz diorite at Sierrita. 'Early' and 'Late' refer to relative ages of veins, 'Wall' and 'Center' refer to early and later mineral assemblages, respectively, within each vein. Capitalized mineral abbreviations indicate relative abundance of the mineral in the assemblage, while lower case abbreviations indicate minor or trace amounts of the mineral.

Wall ——————————————————————————→ Center

Early ↓ Late	Vein	Mineralogy	Fluid Inclusion: T_H (°C)	Salinity (molal $NaCl_{eq}$)	Vein	Mineralogy	Fluid Inclusion T_H (°C)	Salinity (molal $NaCl_{eq}$)
	BQD-2A	Qtz, Bio, an, or, anh, ser	325	12	Qtz, Epid, Chl, py, cpy		390	2
	BQD-2B	Qtz, Bio, An, Or, Anh (ser)	410	2	Qtz, Epid, Py, Cpy, chl, mgt, hem		390	3
	BQD-2C	Qtz. Bio, An, Or, Ser	375	2	Qtz, Epid, Chl, Py Cpy, Anh, mo, mgt		340	2
	BQD-2D	Qtz, Bio, An, Or, anh, ser	360	2	Epid, Qtz, Cpy, Py, Anh, mo, mgt, chl, ser		320	2
	BQD-2E	Qtz, Bio, An Anh, Or, ser	325	2	Epid, Qtz, Cpy, Py, chl, mgt, mo, anh, ser		310	3

Vein Studied; (in this paper)

Mineralogy	T_H (°C)	Salinity (molal $NaCl_{eq}$)
Qtz, Epid, Cpy, Py, anh, mgt, mo	320	1

sample. Temperatures were recorded by a chromel - alumel thermocouple connected to a digital readout display with a 0.1°C resolution. Thermal gradients within the 2.5 cm sample chamber were found to be less than 10°C. The effect of this thermal variation was minimized by using small (less than 0.5 cm) sample chips and by placing the thermocouple tip directly on the sample as close as practical to the inclusion being analyzed. Freezing temperatures were determined by passing N_2 gas, cooled in liquid nitrogen, over the sample, the temperature being recorded as they were during the heating analyses.

Melting points of commercially available eutectic mixtures of organic compounds and distilled water sealed in capillary tubes were used to calibrate the system. Heating temperatures are considered accurate to ± 5°C while freezing temperatures are accurate to ± 0.2°C over the range of temperatures measured in this study. The largest source for error in these measurements comes from difficulty in seeing the final stages of phase changes in the inclusions. To minimize this problem, only heating data reproducible to within 5°C and freezing data reproducible to within 0.2°C were accepted.

Preece and Beane (1982) documented a general decrease in temperature of hydrothermal fluids with time at Sierrita as illustrated by the homogenization temperatures of 'primary' fluid inclusions summarized in Table 3. The exception of this trend is the increase in homogenization temperatures during the transition from early hypersaline to later more dilute fluids (vein BQD 2A). Preece and Beane further noted that later hydrothermal events were commonly

recorded as secondary fluid inclusions in earlier formed vein quartz. It was their conclusion that the highest temperature inclusions found in a given vein represented the temperature of formation of that vein unless the early hypersaline fluids were involved. This principle has been applied to the determination of the homogenization temperatures of inclusions in this study. No attempt has been made to distinguish between 'primary', 'secondary' or 'pseudo-secondary' inclusions based on morphology, a distinction which is often difficult to make in veins from porphyry copper deposits (Nash, 1975).

In order to screen out the numerous low temperature secondary fluid inclusions in the quartz, individual polished quartz chips were examined at 250°C in order to locate inclusions which had not yet homogenized at this temperature. When found in a chip, one higher homogenization temperature inclusion only was analyzed, and that measurement repeated, to ensure against errors resulting from leakage or decrepitation. The freezing point depression of that inclusion was then measured twice.

The homogenization temperatures in excess of 250°C measured in this study are shown in Figure 3. The distinct grouping between 310 and 330°C, averaging approximately 320°C, is interpreted to represent the 'primary' vein-filling solution temperature. The freezing point depression measured for these inclusions averaged, with only minior variation, -3.5°C. According to Potter, et al (1977), this corresponds to a salinity of 1.14 molal NaCl equivalent.

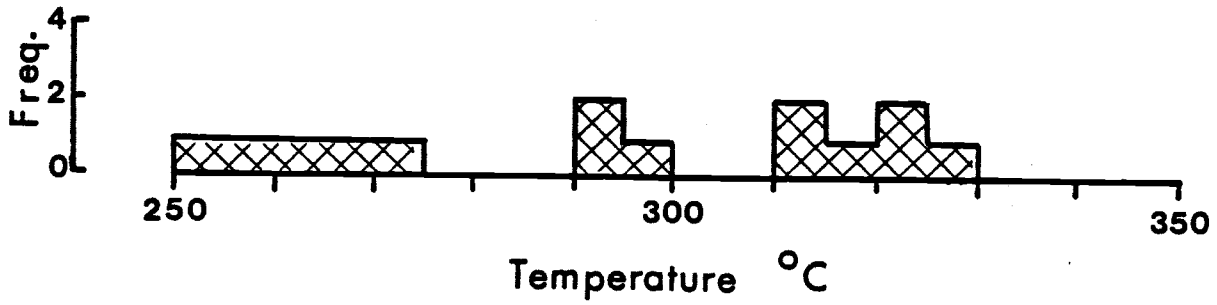

Figure 3. Fluid inclusion homogenization temperatures from the vein studied.

Only inclusions with T_H greater than 250°C were analyzed. The average freezing point depression of the six highest temperature (310-330°C) inclusions was -3.6°C.

From indications of boiling in the fluid inclusions from one sample, Preece and Beane (1982) inferred a pressure of formation of that vein to be 330 bars. Lacking such boiling relationships in the vein selected for this study, or any further indications of pressure in the literature, it is assumed that pressure during the time of formation of the vein studied was also 330 bars.

At 330 bars pressure, the correction to the homogenization temperature of 320°C for a 1 molal NaCl equivalent fluid is +25°C. This implies a temperature of formation of the vein of 345°C. For the purposes of this study a temperature of 350°C will be used as the temperature of formation in all subsequent calculations. The measured homogenization temperature and salinity correlates with the later 'propylitic' stage of Preece and Beane's vein BQD 2D which exhibits a comparable mineralogy (see Table 3).

Mineral Compositions

Several of the minerals in the vein-filling and wall rock assemblages are solid solutions whose compositions can not be safely assumed to be end-member compositions. Of particular importance to this study are the compositions of the feldspars and epidotes, as the compositions of these minerals have a dramatic effect on the activity of their end-member components. These compositions were determined by electron microprobe analyses. Equipment, procedures and results are described in Appendix A.

Fifteen wall rock feldspars were analyzed and the results plotted on a $KAlSi_3O_8$ - $NaAlSi_3O_8$ - $CaAl_2Si_2O_8$ ternary diagram (Fig. 4). These results are similar to those obtained by Preece and Beane (1982) for selvage feldspars. The cluster of analyses about Or_2, Ab_{60}, An_{38} is interpreted to represent the composition of the igneous plagioclase from the biotite quartz diorite. A distinct compositional break occurs between these igneous feldspars and the more alkali-rich feldspars which contain only 5-10 mole% An component. These low An feldspars are interpreted to be alkali-altered plagioclases. The general tendency for the alkali-rich feldspars to be near the vein and the more calcic ones to lie further into the wall rock was noted during the analyses and taken to indicate that the vein-forming fluids were responsible for the alteration of these plagioclases.

The large range in the Na and K contents of the alkali feldspars is probably not representative of equilibrium partitioning of these elements at vein-filling temperatures. The two alkali feldspar compositions with Or concentrations in excess of 10 mole % are theoretically impossible for feldspars formed, or equilibrated, at or near 350°C (Parsons, 1978). The scatter in the Na and K contents and the disequilibrium feldspar compositions are interpreted to be the result of the width of the electron beam relative to the thickness of perthite lamellae. The electron beam probably measured bulk, or weighted average, compositions of Na- and K- rich lamellae of two compositionally distinct feldspars. The compositions of these two

Figure 4. $KAlSi_3O_8$ - $NaAlSi_3O_8$ - $CaAl_2Si_2O_8$ ternary plot of vein selvage feldspar compositions as determined by SEMQ analyses.

The two tick marks along the $KAlSi_3O_8$ - $NaAlSi_3O_8$ join indicate the composition of the alkali feldspar solvus at 350°C.

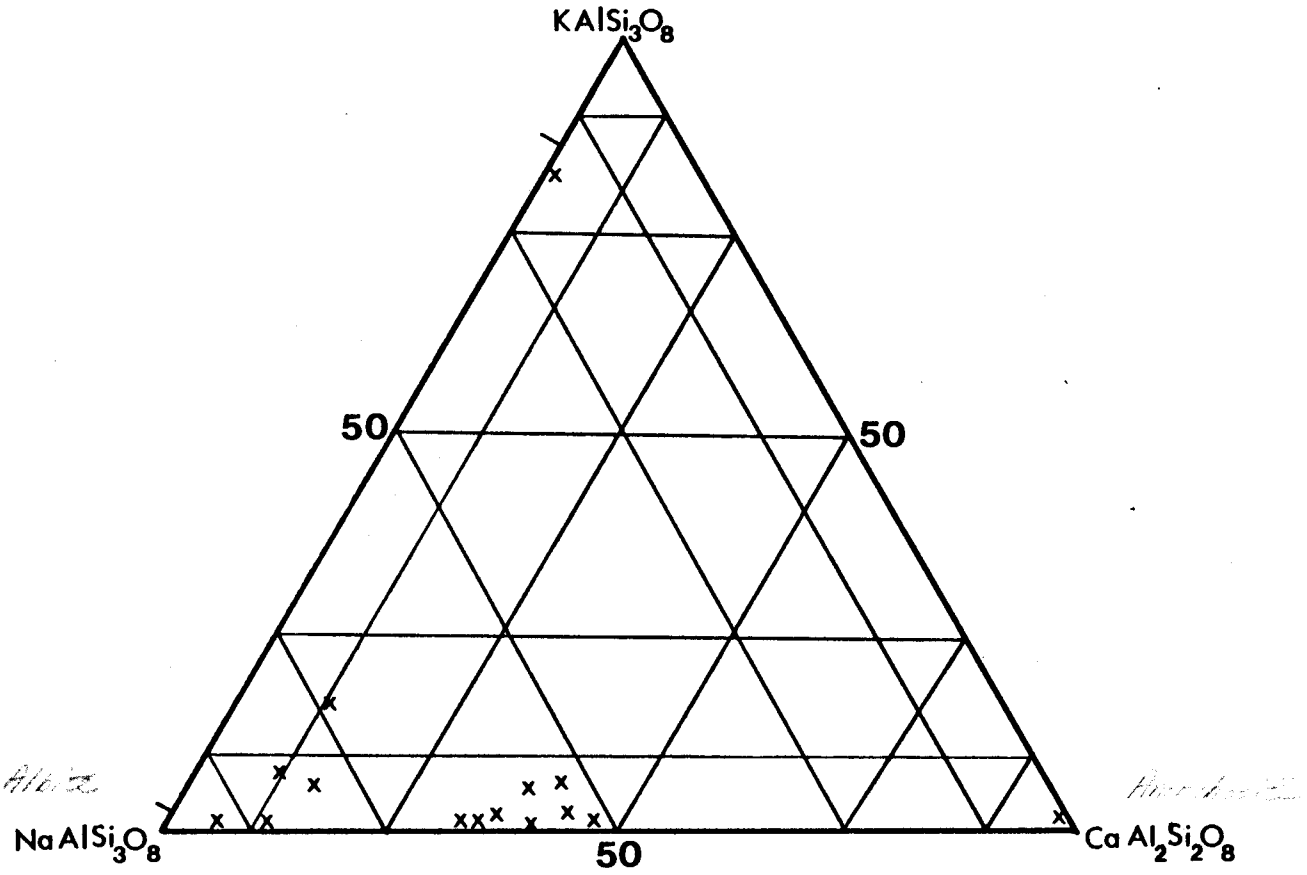

Figure 4. $KAlSi_3O_8$ - $NaAlSi_3O_8$ - $CaAl_2Si_2O_8$ ternary plot of vein selvage feldspar compositions as determined by SEMQ analyses.

equilibrium feldspars should lie on the alkali feldspar solvus for the temperature at which they equilibrated. Figure 5 is a diagram showing the solvus compostions for the alkali feldspars as a function of temperature. At 350°C the equilibrium solvus compositions are Or_{87}, Ab_{13} and Or_2, Ab_{98}. Figure 5 applies to pure alkali feldspars only; the effects of calcium on the solvus compositions are not considered. For alkali feldspar compositions more Or-rich than about $X_{Or} = 0.5$, the maximum An content is less than 2 mole % (Saxena, 1973) which will have only a minor affect on the Or concentration in such a feldspar. However, An concentrations in high Ab alkali feldspars can be significant (in this study around 10 mole %, see Fig. 4). The data necessary for the calculation of the activity - composition relationship of ternary feldspars are not available. It is therefore necessary to assume ideal mixing behaviors between the Ab-rich alkali feldspar and the contained An component. This assumption yields a mixture of an alkali feldspar with a composition of Or_2, Ab_{98} and a calcic feldspar, An_{100}, of $(Or_2, Ab_{98})_{0.9}(An_{100})_{0.1}$. The Ab content of such a mixture is 0.88. The composition of alkali feldspars to be used in this study are Or_{87}, Ab_{13} for the potassium-rich feldspar and Or_2, Ab_{88}, An_{10} for the sodium-rich feldspar.

Twenty-six epidote analyses, from both vein-center and selvage epidotes, are plotted in Figure 6. The results fall into two distinct groups on either side of the ideal epidote composition, $Ca_2FeAl_2Si_3O_{12}(OH)$, in the clinozoisite - pistacite solid solution series. The significance of this bimodal distribution of epidote

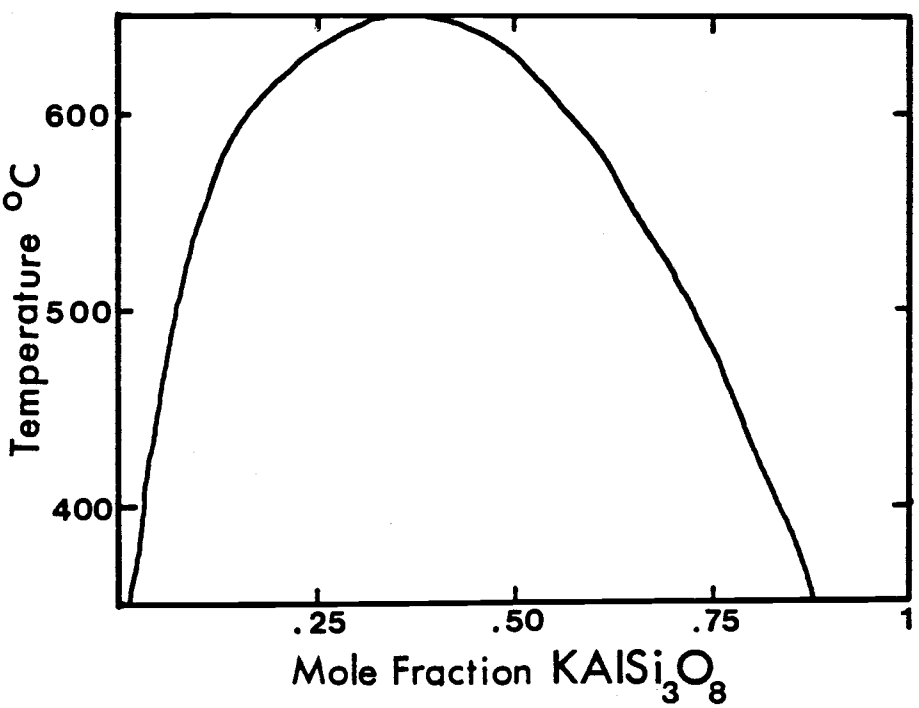

Figure 5. Equilibrium alkali feldspar solvus compositions as a function of temperature.

From Parsons, 1978.

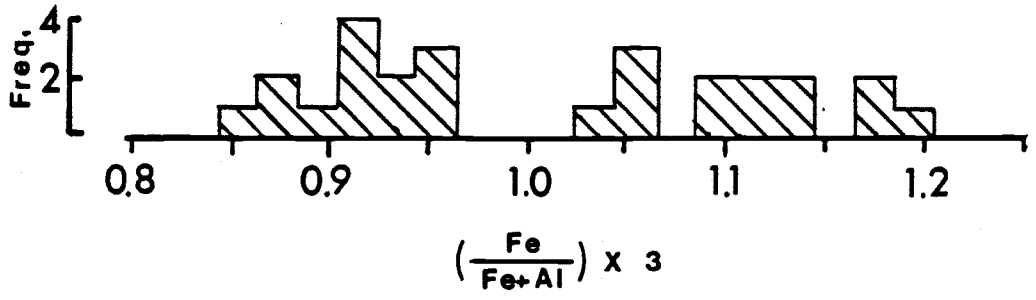

Figure 6. Compositions of vein and wall rock epidotes as determined by SEMQ analyses.

The results are plotted as mole fraction $\frac{Fe}{Fe + Al} \times 3$.

compositions is not known. In his study of epidote compositions at Sierrita, Fellows (1976) reports a similar bimodal distribution of epidote compositions for which no explanation is offered. Thermodynamic data for epidote compositions more iron-rich than ideal epidote are limited and suspect while reliable data are available only for compositions in the clinozoisite - epidote range (D. Bird, pers. comm., 1982). Therefore, the composition of 'epidote' used in this study is taken from the lower-iron set of analyses. The average composition of this group is; $X_{epid} = 0.915$, $X_{clino} = 0.085$.

Because the vein sulfides pyrite and chalcopyrite were complexly intergrown, it was not possible to physically separate the two minerals for sulfur isotope analysis. Therefore, a mixed pyrite + chalcopyrite sample was extracted from the vein by hand, crushed to a fine powder, homogenized and split into six samples. Five of these were reserved for mass spectrometric analysis. The sixth was analyzed for its copper to iron ratio which was used to calculate the original chalcopyrite to pyrite ratio in the powder. The small amount of magnetite present in the sulfides was removed with a magnet. The sample was then fused in a molybdenum strip furnace in order to create a thoroughly homogenized pellet. Some of the sulfur was lost during this process, but the iron and copper, which have very low vapor pressures, remained and were combined into a single phase. After rapid quenching, the resulting pellet was analyzed for its copper, iron and sulfur contents. Sixteen spot analyses indicated a molar copper to iron ratio of 0.305 : 0.695. Since pyrite and chalcopyrite

were the only minerals in the sulfide powder, the measured atomic ratio indicates a molar chalcopyrite to pyrite ratio of 0.44 : 0.56 (assuming stoichiometric compositions for pyrite and chalcopyrite).

Sulfur Isotopic Analyses

The isotopic compositions of sulfide minerals were determined at the University of Arizona's Laboratory of Isotope Geochemistry on a 602C Micromass mass spectrometer relative to a standard SO_2 gas of known isotopic composition. Both SO_2 and SO were analyzed so that it was possible to account for the isotopic composition of oxygen in the gases. The resulting data were reduced on a TRS-80 computer using a program written by D. Steinke and A. Long of the University of Arizona.

The five powdered pyrite + chalcopyrite samples visually estimated to be > 95% sulfide were extracted from the vein, combined with excess amounts of an oxidant (tenorite), placed in a vacuum system and heated to in excess of 900°C. This process liberated the sulfur from the sulfide phase and combined it with oxygen to form SO_2 gas. The gas was isolated from potential contaminants (O_2, CO_2, H_2O, etc.) and collected. The sulfur isotopic compositions of the five sulfide samples are listed in Table 4. The average of these values, which ranged from -1.86 to -0.76‰, is -1.33‰

A sample of vein-filling anhydrite was extracted from the vein. Binocular microscope examination indicated that the sample contained less than 2% sulfide contamination. The sulfur isotopic

Table 4. Measured $\delta^{34}S$ values, as determined by mass spectrometric analyses, of the mixed sulfide and anhydrite samples.

Mixed sulfide sample:

Sample #	A	B	C	D	E
$\delta^{34}S$(°/oo)	-0.92	-1.79	-1.86	-1.31	-0.76

Vein anhydrite:

$\delta^{34}S$ = +8.8 °/oo

analysis of the anhydrite was performed by Geochron Laboratories in Cambridge, Massachusetts. The $\delta^{34}S$ value of the anhydrite was determined to be $+8.8^{o}/oo$.

CALCULATION OF SOLUTION COMPOSITION

Based on the assumption of chemical equilibrium between the vein-filling and alteration mineral assemblages and the mineralizing solution, necessary chemical parameters of the solution were derived using mineral stability calculations. The vein-filling assemblage of quartz, epidote, anhydrite, pyrite and magnetite fixes the oxygen fugacity of the system. The presence of two alkali feldspars in the wall rock alteration assemblage allows the ratio of aqueous Na^+ to K^+ to be fixed, which in conjunction with the salinity of the fluid allows the activities of both species to be calculated. The pH of the solution is bracketed by the sericite - potassium feldspar and epidote - garnet buffers, while a reaction written between epidote and sodium feldspar can be employed to fix the pH within those limits. Another epidote - feldspar reaction can be used to define the Ca^{2+} activity. These calculations will all be described and discussed in detail below. It is important to note that all reactions to be employed in fixing these chemical parameters involve mineral assemblages present in this single vein.

The reaction constants used in these calculations are the 'thermodynamic equilibrium reaction constants' of Garrels and Christ (1965). The activities of pure solids are defined as unity. Minerals not known to have significant impurities have been assigned activities of one for use in the following calculations. In this study, these

minerals include: anhydrite, chalcopyrite, hematite, magnetite, pyrite and quartz. Sericite (muscovite) is known to contain significant impurities. However, it was present in such fine grains in the sample that SEMQ analysis was precluded. Sericite was therefore arbitrarily assigned an activity of one. The activity of H_2O in a 1 molal NaCl equivalent solution at 350°C is calculated by Helgeson (1968) to be 0.98.

Oxygen Fugacity

General constraints on oxygen fugacity in the fluid can be drawn from the presence of magnetite and the general absence of hematite in the alteration assemblage of the biotite quartz diorite, while hematite appears to be the stable iron oxide phase in the Harris Ranch quartz monzonite alteration assemblage (Preece and Beane 1982). As the sample for this study came from very near the contact (less than 25 m, see Fig. 2) of these two units, the oxygen fugacity of the fluid can reasonably be expected to be close to the value for the hematite-magnetite oxygen buffer. The equilibrium f_{O_2} for this buffer can be calculated from the equilibrium constant, K_{30}, for the reaction:

$$\underset{\text{(hem)}}{3\ Fe_2O_3} = \underset{\text{(mgt)}}{2\ Fe_3O_4} + 1/2\ O_2 \qquad (30)$$

where:

$$K_{30} = \frac{(f_{O_2})^{1/2} (a_{mgt})^2}{(a_{hem})^3} \qquad (31)$$

from which the oxygen fugacity is defined as:

$$\log f_{O_2} = 2 \log K_{30} \qquad (32)$$

Substituting the reaction constant K_{30} from Table 5 in Equation 32 yeilds an equilibrium oxygen fugacity of $\log f_{O_2} = -27.4$, magnetite being the stable iron oxide at lower values. This value represents an upper limit on the fugacity of oxygen.

A direct measure of the oxygen fugacity comes from a reaction between the observed vein-filling minerals:

$$\underset{\text{(epid)}}{18\ Ca_2FeAl_2Si_3O_{12}(OH)} + \underset{\text{(py)}}{6\ FeS_2} + 20.5\ O_2 = \qquad (33)$$

$$\underset{\text{(clino)}}{12\ Ca_2Al_3Si_3O_{12}(OH)} + \underset{\text{(anh)}}{12\ CaSO_4} + \underset{\text{(qtz)}}{18\ SiO_2} + \underset{\text{(mgt)}}{8\ Fe_3O_4} + 3\ H_2O$$

from which:

Table 5. Equilibrium constants for reactions given in the text. a) from the data of Helgeson et. al. (1978); b) from Barnes (1979).

#	Reaction	log K at 350°C and 330 bars	Reference
8	$H_2S^\circ = HS^- + H^+$	-8.9	a,b
9	$H_2S^\circ = S^{2-} + 2\ H^+$	-21.0	a,b
10	$H_2S^\circ + 2\ O_2 = SO_4^{2-} + 2\ H^+$	+39.4	a
11	$H_2S^\circ + 2\ O_2 = HSO_4^- + H^+$	+47.9	a
12	$H_2S^\circ + 2\ O_2 + Na^+ = NaSO_4^- + 2\ H^+$	+39.2	a
13	$H_2S^\circ + 2\ O_2 + K^+ = KSO_4^- + 2\ H^+$	+42.9	a
14	$H_2S^\circ + 2\ O_2 + Ca^{2+} = CaSO_4^\circ + 2\ H^+$	+44.7	a
30	$3\ Fe_2O_3 = 2\ Fe_3O_4 + 0.5\ O_2$	-13.7	a
33	$18\ Ca_2FeAl_2Si_3O_{12}(OH) + 6\ FeS_2 + 20.5\ O_2 =$ $12\ Ca_2Al_3Si_3O_{12}(OH) + 12\ CaSO_4 + 18\ SiO_2 +$ $8\ Fe_3O_4 + 3\ H_2O$	+553.2	a
38	$NaAlSi_3O_8 + K^+ = KAlSi_3O_8 + Na^+$	+0.8	a
45	$3\ KAlSi_3O_8 + 2\ H^+ =$ $KAl_3Si_3O_{10}(OH)_2 + 6\ SiO_2 + 2\ K^+$	+7.6	a

Table 5 - continued

#	Reaction	log K at 350°C and 330 bars	Reference
48	$84\ Ca_2Al_3Si_3O_{12}(OH) + 306\ SiO_2 + 10\ Fe_3O_4 + 2.5\ O_2 + 120\ Na^+ + 33\ H_2O =$ $36\ Ca_3Al_2Si_3O_{12} + 30\ Ca_2FeAl_2Si_3O_{12}(OH) + 120\ NaAlSi_3O_8 + 120\ H^+$	+500.6	a
51	$6\ Ca_2FeAl_2Si_3O_{12}(OH) + 6\ NaAlSi_3O_8 + 6\ H^+ =$ $6\ Ca_2Al_3Si_3O_{12}(OH) + 18\ SiO_2 + 2\ Fe_3O_4 + 6\ Na^+ + 0.5\ O_2 + 3\ H_2O$	+8.6	a
54	$12\ Ca_2FeAl_2Si_3O_{12}(OH) + 32\ H_2S^\circ + 19\ O_2 =$ $8\ Ca_2Al_3Si_3O_{12}(OH) + 12\ FeS_2 + 8\ CaSO_4 + 12\ SiO_2 + 34\ H_2O$	+147.3	a
58	$CaSO_4\ (anh) = Ca^{2+} + SO_4^{2-}$	-11.7	a

$$K_{33} = \frac{(a_{clino})^{12} (a_{anh})^{12} (a_{qtz})^{18} (a_{mgt})^{8} (a_{H_2O})^{3}}{(a_{epid})^{18} (a_{py})^{6} (f_{O_2})^{20.5}} \quad (34)$$

The fugacity of oxygen is then defined by:

$$\log f_{O_2} = \frac{1}{20.5} [12 \log a_{clino} + 3 \log a_{H_2O} - 18 \log a_{epid} - \log K_{33}] \quad (35)$$

The activities of clinozoisite and epidote can be calculated from the composition of the solid solution as determined by SEMQ analysis using the activity-composition relationships for this solid solution series given by Bird and Helgeson (1980) in Figure 7. From these relationships and the measured composition of vein epidotes of X_{epid} = 0.915, the activities of clinozoisite and epidote in this system are found to be 0.12 and 0.95, respectively. Substituting these values for the activities of clinozoisite and epidote and the reaction constant for Reaction 33 (Table 5) into Equation 35 yields $\log f_{O_2}$ = -27.5. This is close to the magnetite-hematite buffer and satisfies the requirement for magnetite stability discussed above.

Activities of Na^+ and K^+

Neither fluid inclusion analyses nor equilibrium mineral stability relationships alone are sufficient to determine the

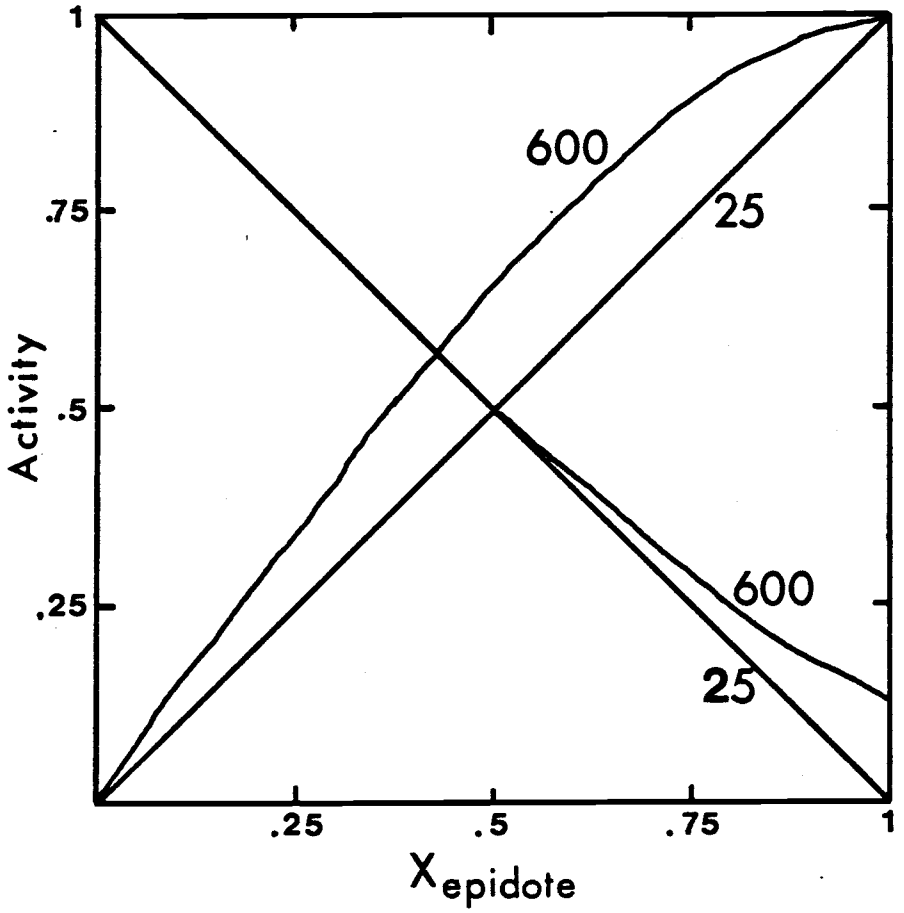

Figure 7. Activity - composition relationships of epidote and clinozosite in the epidote solid solution series.

Contours show the activity - composition relationships at 25 and 600°C. From Bird and Helgeson, 1980.

activities of the Na^+ and K^+ ions in the mineralizing solution. However, salinity data from fluid inclusion studies provide information on the total molality of Na and K in solution, while the alkali feldspar assemblage serves to fix the activity ratio of Na^+ : K^+. Taken together, this information can be used to calculate the absolute activities of both Na^+ and K^+.

From the measured freezing point depression in fluid inclusions, a salinity of 1.14 molal NaCl equivalent was determined for the mineralizing fluids. It has been shown that the salinity of hydrothermal solutions in general and of porphyry copper deposits in particular are dominated by NaCl and KCl (Roedder, 1979, 1972; Dennis, 1974). Since the effect on the aqueous freezing point depression of NaCl + KCl solutions is nearly identical to that of pure NaCl solutions (Potter, 1977), the NaCl equivalent salinity may be very closely approximated by:

$$1.14 = m_{NaCl} + m_{KCl} \tag{36}$$

which in turn implies that:

$$1.14 = m_{Na} + m_{K} \tag{37}$$

Based on the presence of two coexisting alkali feldspars in the vein selvage, as indicated by the SEMQ analysis, the following reaction can be written:

(Ab) (Or)

$$NaAlSi_3O_8 + K^+ = KAlSi_3O_8 + Na^+ \quad (38)$$

where:

$$K_{38} = \frac{(a_{Or})\ (a_{Na^+})}{(a_{Ab})\ (a_{K^+})} \quad (39)$$

from which the activity ratio of Na^+ to K^+ is defined by:

$$\frac{(a_{Na^+})}{(a_{K^+})} = \frac{(K_{38})\ (a_{Ab})}{(a_{Or})} \quad (40)$$

This activity ratio of Na^+ to K^+ can be converted to a molar ratio of Na to K in solution through the stoichiometric ion activity coefficient, $\dot{\gamma}$:

$$a_i = m_{\Sigma i} \cdot \dot{\gamma}_i \quad (41)$$

where 'i' is an ion of an element and '$m_{\Sigma i}$' is the total molalilty of that element in solution (both free and associated). The $\dot{\gamma}$ for any given ion in solution is a function of temperature, pressure, solution composition and properties of the individual ion (size and charge) (Garrels and Christ, 1965). Helgeson (1974, 1969) has tabulated values of $\dot{\gamma}$ for Na^+ and K^+ in aqueous solutions for various NaCl concentrations at temperatures up to 300°C. Above 300°C, the

thermodynamic data for species in concentrated solutions are not well known. It was therefore necessary to extrapolate the $\dot{\gamma}$'s reported by Helgeson (1974) up to 350°C. Although values of $\dot{\gamma}$ for Na^+ and K^+ begin to change significantly at and above 300°C in concentrated chloride solutions, the ratio of $\dot{\gamma}_{Na^+}$ to $\dot{\gamma}_{K^+}$ changes more slowly with increasing temperature and is hence more acceptable for extrapolation at 350°C. For a 350°C and 1 molal NaCl equivalent solution, the extrapolated $\dot{\gamma}_{Na^+}$: $\dot{\gamma}_{K^+}$ ratio is 0.89. The individual $\dot{\gamma}$'s for Na^+ and K^+ are estimated to be 0.063 and 0.071, respectively. The error involved in these extrapolations can not be readily estimated.

Substituting the relationships between activity and molality (Equation 41) and the activity coefficient ratio of these species (0.89) into Equation 40 gives an equation defining the molar ratio of Na : K in solution:

$$\frac{m_{Na}}{m_K} = \frac{(K_{38})(a_{Ab})}{(a_{Or})(0.89)} \qquad (42)$$

The results of the SEMQ analysis of vein selvage feldspars indicate the presence of two coexisting alkali feldspars. The compositions of these are interpreted to be Or_{87}, Ab_{13}, and Or_2, Ab_{88}, An_{10} for the potassium- and sodium- rich alkali feldspars, respectively. Waldbaum and Thompson (1969) have calculated the activity-composition relationships for the alkali feldspars and their results are summarized in Figure 8. At temperatures near 350°C it is

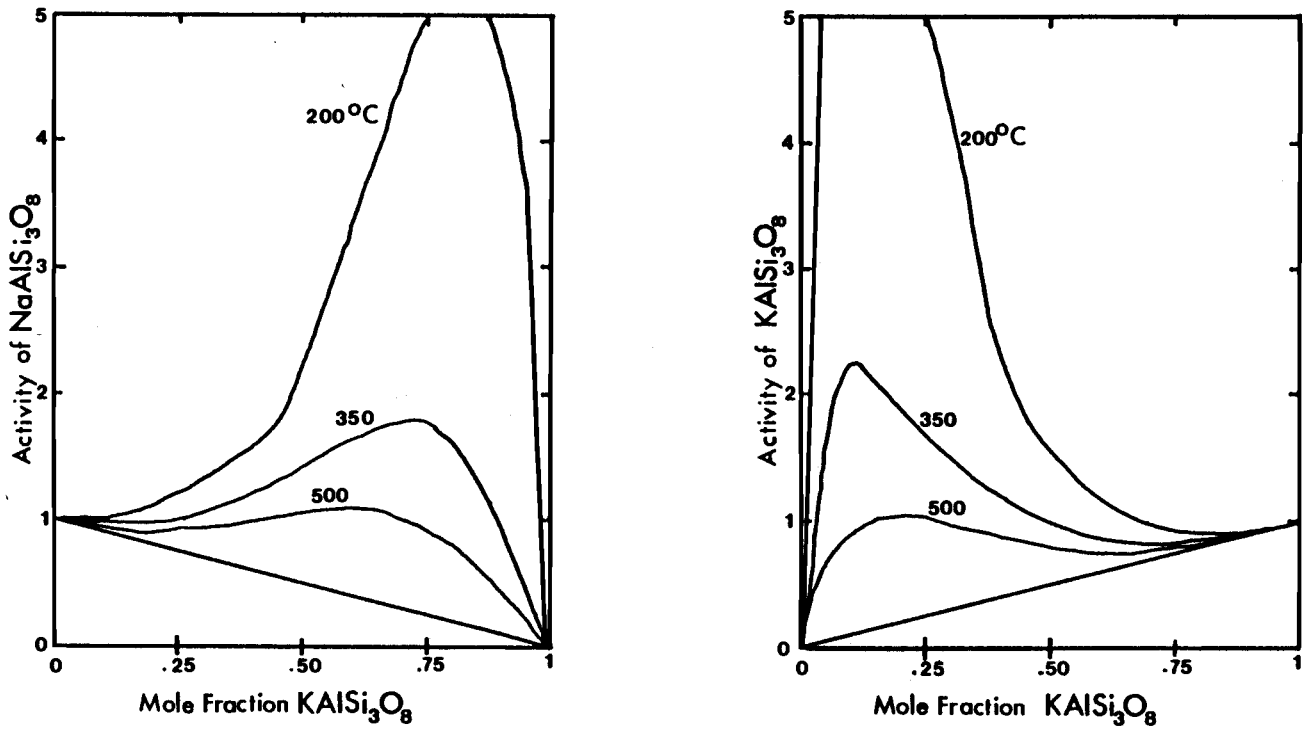

Figure 8. Activity - composition relationships of alkali feldspars.

Contours indicate the activity - composition relationships at 200, 350 and 500°C. From Waldbaum and Thompson, 1969.

apparent that the activities of both end-members digress dramatically from a Raoult's Law approximation at low concentrations of that end-member feldspar. However, when the end-member component's concentration is greater than approximately 0.8, Raoult's Law approximation is fairly accurate. In addition, temperature has only a minor effect on the calculated activities.

Employing the equilibrium condition that the activity of a species is equal in all phases in which it is present gives:

$$a_{Ab}^{\text{K-rich feldspar}} = a_{Ab}^{\text{Na-rich feldspar}} \tag{43}$$

$$a_{Or}^{\text{K-rich feldspar}} = a_{Or}^{\text{Na-rich feldspar}} \tag{44}$$

where a_x^y is the activity of component 'x' in mineral 'y'. The activity of each of the end-member components can be calculated from the solvus composition at which that component represents more than 0.8 of the feldspar. This yields activities of 0.94 for the sodium end-member and 0.90 for the potassium end-member. Substituting these values and the appropriate reaction constant from Table 5 into Equation 42 yields a molar ratio Na : K = 7.40. Combining this ratio with Equation 37 results in two equations and two unknowns which, when solved simultaneously, yields 1.01 moles Na and 0.13 moles K in solution. The individual $\dot{\gamma}$'s for Na^+ and K^+ discussed above can be used to convert these molalities to activity of $Na^+ = 6.3 \times 10^{-2}$ and activity of $K^+ = 9.8 \times 10^{-3}$.

Solution pH

Upper and lower limits on the activity of the H^+ ion, or pH, were established based on the presence and absence of certain minerals in the observed assemblages. Sericite was observed in the wall rock assemblage, but its place in the paragenetic sequence is not certain. In particular, the possibility that this sericite is the product of a weak 'phyllic overprint' can not be ruled out. However, potassium feldspar is present in the wall rock alteration assemblage, and its presence implies that the equilibium pH did not fall below the limit imposed by the reaction:

$$\underset{(Or)}{3\ KAlSi_3O_8} + 2\ H^+ = \underset{(ser)}{KAl_3Si_3O_{10}(OH)_2} + \underset{(qtz)}{6\ SiO_2} + 2\ K^+ \qquad (45)$$

where:

$$K_{45} = \frac{(a_{ser})\ (a_{qtz})^6\ (a_{K^+})^2}{(a_{Or})^3\ (a_{H^+})^2} \qquad (46)$$

The equilibrium pH, at a fixed activity of K^+, is defined by:

$$\log a_{H^+} = 0.5 \log a_{ser} + \log a_{K^+} - 1.5 \log a_{Or} - 0.5 \log K_{45} \qquad (47)$$

Substituting the activities of potassium feldspar and K^+ as well as the reaction constant, K_{45}, from Table 5 into Equation 47 fixes the

minimum pH for this system at 5.8. A lower solution pH would correspond to destruction of potassium feldspar to form sericite.

Similarly, the absence of a Ca - Fe - Al garnet phase in the vein-filling assemblage sets a maximum limit on pH, from the reaction:

$$\underset{\text{(clino)}}{84\ Ca_2Al_3Si_3O_{12}(OH)} + \underset{\text{(qtz)}}{306\ SiO_2} + \underset{\text{(mgt)}}{10\ Fe_3O_4} + \quad (48)$$

$$2.5\ O_2 + 120\ Na^+ + 33\ H_2O =$$

$$\underset{\text{(gr)}}{36\ Ca_3Al_2Si_3O_{12}} + \underset{\text{(epid)}}{30\ Ca_2FeAl_2Si_3O_{12}(OH)} +$$

$$\underset{\text{(Ab)}}{120\ NaAlSi_3O_8} + 120\ H^+$$

where:

(49)

$$K_{48} = \frac{(a_{gr})^{36}\ (a_{epid})^{30}\ (a_{Ab})^{120}\ (a_{H^+})^{120}}{(a_{H_2O})^{33}\ (a_{clino})^{84}\ (a_{qtz})^{306}\ (a_{mgt})^{10}\ (f_{O_2})^{2.5}\ (a_{Na^+})^{120}}$$

This equation places a maximum limit on pH defined by:

$$\log a_{H^+} = \frac{1}{120}[\log K_{48} + 84 \log a_{clino} + 2.5 \log f_{O_2} + 120 \log a_{Na^+} + 33 \log a_{H_2O} - 36 \log a_{gr} - 30 \log a_{epid} - 120 \log a_{Ab} - \log a_{H^+}] \quad (50)$$

The activities of all species involved in Equation 50 except grossular garnet have previously been calculated. The activity of grossular garnet can be derived from the composition of the epidote with which it would have had to have been in equilibrium as described by Bird and Helgeson (1980). The activity of the grossular component of the grandite garnet which would be in equilibrium with the composition of epidote in this study ($X_{epid} = 0.915$) at 350°C is $a_{gr} = 0.068$.

When this value and the other known parameters are substituted into Equation 50, a maximum solution pH is defined at 6.6. A pH larger than this value would require the stabilization of a garnet phase which was not observed in the sample.

A reaction which directly provides pH is:

$$\underset{\text{(epid)}}{6\ Ca_2FeAl_2Si_3O_{12}(OH)} + \underset{\text{(Ab)}}{6\ NaAlSi_3O_8} + 6\ H^+ = \quad (51)$$

$$\underset{\text{(clino)}}{6\ Ca_2Al_3Si_3O_{12}(OH)} + \underset{\text{(qtz)}}{18\ SiO_2} + \underset{\text{(mgt)}}{2\ Fe_3O_4} + 6\ Na^+$$

$$+ 0.5\ O_2 + 3\ H_2O$$

where:

$$K_{51} = \frac{(a_{clino})^6 (a_{qtz})^{18} (a_{mgt})^2 (a_{Na^+})^6 (f_{O_2})^{0.5} (a_{H_2O})^3}{(a_{epid})^6 (a_{Ab})^6 (a_{H^+})^6} \quad (52)$$

The equilibrium pH defined by this reaction is given by:

$$\log a_{H^+} = 1/6[6 \log a_{clino} + 6 \log a_{Na^+} + 0.5 \log f_{O_2} + 3 \log a_{H_2O} - \log K_{51} - 6 \log a_{epid} - 6 \log a_{Ab}] \quad (53)$$

The activities of each of the terms on the right side of Equation 53 have been calculated above. Substituting these and the reaction constant K_{51}, from Table 5 into Equation 53 yields an equilibrium pH = 5.8. The pH calculated by this reaction (5.8) is in agreement with the limiting conditions previously calculated (5.8 - 6.6). A further aspect of this direct pH calculation is that it is identical to that for the limiting Equation 45. Thus sericite is indicated to be a stable part of the equilibrium wall rock assemblage at the time of mineralization and not necessarily the product of a later 'phyllic overprinting'. The pH of the mineralizing solution seems to have been controlled by the alkali feldspar - sericite pH buffer.

Activities of $H_2S°$, SO_4^{2-} and Ca^{2+}

The activity of $H_2S°$ can be defined by the reaction:

$$12\ Ca_2FeAl_2Si_3O_{12}(OH)_{(epid)} + 32\ H_2S° + 19\ O_2 = \quad (54)$$

$$8\ Ca_2Al_3Si_3O_{12}(OH)_{(clino)} + 12\ FeS_{2\ (py)} + 8\ CaSO_{4\ (anh)} + 12\ SiO_{2\ (qtz)}$$

$$+ 34\ H_2O$$

where:

$$K_{54} = \frac{(a_{clino})^8\ (a_{py})^{12}\ (a_{anh})^8\ (a_{qtz})^{12}\ (a_{H_2O})^{34}}{(a_{epid})^{12}\ (a_{H_2S^o})^{32}\ (f_{O_2})^{19}} \quad (55)$$

The activity of aqueous $H_2S°$ is given by:

$$\log a_{H_2S°} = 1/32[8 \log a_{clino} + 34 \log a_{H_2O} - 12 \log a_{epid} - 19 \log f_{O_2} - \log K_{54}] \quad (56)$$

Substituting the previously calculated values for each of the terms

and the reaction constant, K_{54}, from Table 5 into the right side of Equation 56 determines the activity of $H_2S° = 4.80 \times 10^{-3}$.

The activity of SO_4^{2-} in the mineralizing solution can now be calculated from Equation 10:

$$H_2S° + 2\ O_2 = SO_4^{2-} + 2\ H^+$$

From this reaction the activity of SO_4^{2-} is defined by:

$$\log a_{SO_4^{2-}} = \log K_{10} + \log a_{H_2S^o} + 2 \log f_{O_2} - 2 \log a_{H^+} \qquad (57)$$

Substituting the appropriate values determined above into Equation 57 yields an activity of $SO_4^{2-} = 5.13 \times 10^{-7}$.

From this value for the activity of aqueous sulfate and the presence of anhydrite in the vein mineral assemblage, the activity of Ca^{2+} can be calculated. The reaction:

$$CaSO_4\ (anh) = Ca^{2+} + SO_4^{2-} \qquad (58)$$

where:

$$K_{58} = \frac{(a_{Ca^{2+}})\ (a_{SO_4^{2-}})}{(a_{anh})} \qquad (59)$$

provides the activity of Ca^{2+} to be = 1.03×10^{-5} from:

$$\log a_{Ca^{2+}} = \log K_{58} - \log a_{SO_4^{2-}} \qquad (60)$$

RESULTS AND DISCUSSION

Distribution of Aqueous Sulfur

The necessary physical and chemical variables outlined above for the calculation of the distribution of aqueous sulfur have now been determined for the mineralizing solution. These results are summarized in Table 6. The molalities of the remaining aqueous sulfur-bearing species can now be calculated from Equations 15-21. Substituting into these equations the appropriate calculated parameters from Table 6 and the individual ion activity coefficients, γ_i, listed in Table 7, yields the molalities of the aqueous sulfur species as summarized in Table 8. Also presented in Table 8 are the molar percentage of total aqueous sulfur each species represents.

The single most important sulfur-bearing species in solution is H_2S° which accounts for 49.5% of total aqueous sulfur. Other important species are HSO_4^- (37.4%) and SO_4^{2-} (10.8%). Thus sulfur is transported in this solution as nearly equal amounts of sulfide and sulfate.

Figure 9 summarizes graphically the effects of solution chemistry, in particular oxygen fugacity and pH, on the distribution of aqueous sulfur. The calculated f_{O_2} and pH of the solution forming the vein studied have been plotted, along with the hematite-magnetite oxygen buffer and the calculated limits to solution pH. The various fields in Figure 9 depict regions where the labeled species is the

Table 6. A summary of the physical and chemical parameters determined for the vein studied.

Temperature	345°C
Pressure	330 bars
Ionic Strength	1.14
log f_{O_2}	-27.5
$pH_{calculated}$	5.8
minimum	5.8
maximum	6.6
Individual ion activities:	
Na^+	6.3×10^{-2}
K^+	9.8×10^{-3}
Ca^{2+}	1.0×10^{-5}
H_2S°	4.79×10^{-3}
Isotopic Compositions:	
$\delta^{34}S_{pyrite}$	-0.82°/oo
$\delta^{34}S_{anhydrite}$	+ 8.8°/oo

Table 7. Individual ion activity coefficients (γ) and stoichiometric ion activity coefficients ($\mathring{\gamma}$) for the aqueous species in this study in a 350°C and a 1 molal NaCl equivalent solution.

a) from Ohmoto (1974)

b) extrapolated from the data of Helgeson (1969)

c) assumed, this study

Species	log γ	log $\mathring{\gamma}$	reference
H_2S°	+0.35	-	a
HS^-	-0.84	-	a
S^{2-}	-2.64	-	a
SO_4^{2-}	-2.96	-	a
HSO_4^-	-0.77	-	a
$NaSO_4^-$	-0.77	-	a
KSO_4^-	-0.77	-	a
$CaSO_4^\circ$	0	-	c
Ca^{2+}	-1.88	-	a
Na^+	-	-1.20	b
K^+	-	-1.15	b

Table 8. Summary of the molalities, relative distribution and isotopic compositions of aqueous sulfur species determined in this study.

Aqueous Sulfur Species	Molality	Molar %	$\delta^{34}S$(°/oo)
H_2S°	2.14×10^{-3}	49.5	-1.85
HS^-	2.63×10^{-5}	0.6	-2.60
S^{2-}	2.09×10^{-9}	---	-5.59
SO_4^{2-}	4.68×10^{-4}	10.8	+8.8
HSO_4^-	1.62×10^{-3}	37.4	+8.8
$NaSO_4^-$	1.26×10^{-7}	---	+8.8
KSO_4^-	7.25×10^{-5}	1.7	+8.8
$CaSO_4^\circ$	5.01×10^{-7}	---	+8.8
	4.33×10^{-3}	100.0	

Figure 9. Molar predominance diagram for aqueous sulfur species; f_{O_2} vs. pH.

Drawn for a system at 350°C, 330 bars and ionic strength of solution = 1. $NaSO_4^-$, KSO_4^- and $CaSO_4^o$ do not have a field of predominance at the activities of Na^+, K^+ and Ca^{2+} determined in this study (Table 6). The heavy solid lines define regions where the indicated species is the most abundant sulfur-bearing species in solution. The dashed lines indicate the region in each field where the appropriate species makes up greater than 90% of the total aqueous sulfur. Also plotted in this diagram is the hematite-magnetite oxygen buffer and the pH limits calculated for the mineralizing solution in this study.

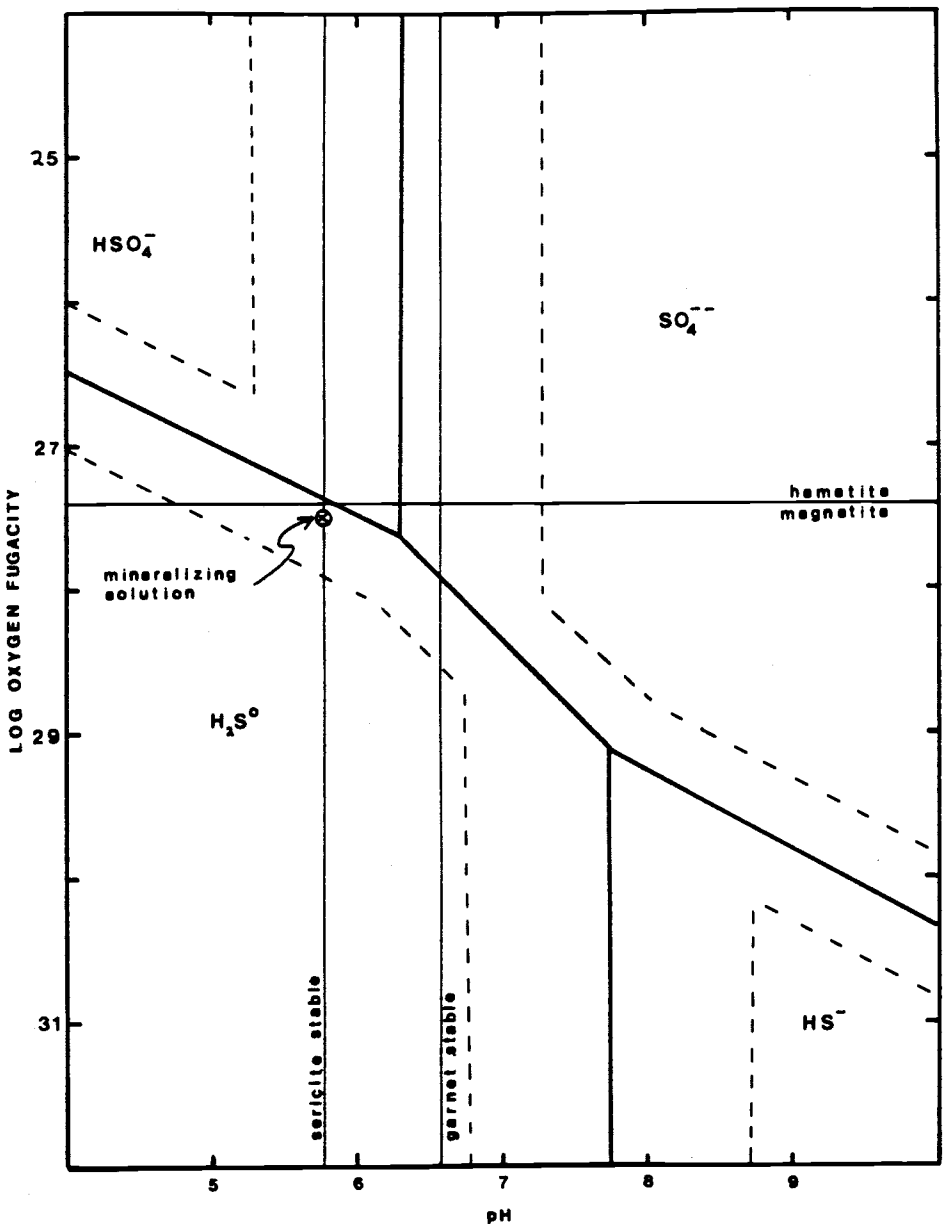

Figure 9. Molar predominance diagram for aqueous species; f_{O_2} vs. pH.

most abundant sulfur-bearing form in solution. As a boundary between two fields is approached, the molar ratio of the two aqueous species changes, as illustrated by the dashed line contours. The solid boundary defining lines indicate equal amounts of the two species in solution. The dashed lines show where the individual species becomes 90% of total aqueous sulfur. Every aqueous sulfur species is present in solution over the entire extent of the diagram, although when solution conditions plot well outside the field of predominance of a given species, its molar fraction in such a solution may be trivially small. The oxygen fugacity and pH calculated in this study define a point in the diagram falling just on the H_2S° side of the H_2S° - HSO_4^- predominance boundary, reflecting the calculated 50 : 37 molar ratio of these two species. Note that small changes (eg., 0.5 log unit) in pH and/or f_{O_2} can have a dramatic affect on the distribution of aqueous sulfur. Such changes may control the timing and style (sulfide vs. sulfate) of mineralization in the system.

Sulfur Isotopic Composition of the Hydrothermal Solution

The sulfur isotopic composition of the hydrothermal pyrites in the studied vein can be calculated from the measured $\delta^{34}S = -1.33^o/_{oo}$ of the mixed sulfide sample. During the SEMQ analysis, it was noted that iron and copper were the only metals present in the sulfide powder in anything but trace quantities. Thus, the isotopic composition of the sulfide powder can be expressed as:

$$\delta^{34}S_{\text{sulfide powder}} = (X_{cpy} \cdot \delta^{34}S_{cpy}) + (X_{py} \cdot \delta^{34}S_{py}) \qquad (61)$$

The mole fractions of chalcopyrite and pyrite were determined by the SEMQ to be 0.44 and 0.56, respectively. The isotopic composition of chalcopyrite can be related to that of pyrite by the equilibrium isotopic enrichment factor, Δ_{cpy-py}. From Equation 2 and the value of Δ_{cpy-py} in Table 9, $\delta^{34}S_{cpy}$ is given by:

$$\delta^{34}S_{cpy} = \delta^{34}S_{py} - 1.16 \qquad (62)$$

Substituting this relation and the appropriate values from above into Equation 61 yields:

$$-1.33 = 0.44(\delta^{34}S_{py} - 1.16) + 0.56(\delta^{34}S_{py}) \qquad (63)$$

from which the isotopic composition of pyrite is calculated to be $-0.82^{o}/oo$. The corresponding isotopic composition of chalcopyrite is $-1.98^{o}/oo$.

The calculation of the $\delta^{34}S$ values of the pyrite and chalcopyrite in the mixed sulfide sample assumes isotopic equilibrium between the two minerals at the fluid inclusion-based temperature of formation of 350°C. The corresponding $\delta^{34}S$ of anhydrite in equilibrium with these sulfides at 350°C is calculated to be $+18.5^{o}/oo$ (Ohmoto and Rye, 1979). This is significantly different than the $\delta^{34}S$ value of $+8.8^{o}/oo$ measured in this study. The temperature at which the

Table 9. The relative sulfur isotopic enrichment factors of the sulfur-bearing aqueous and mineral species in this study (from Ohmoto and Rye, 1979).

$$\Delta_{i\text{-}py} = \delta^{34}S_i - \delta^{34}S_{py}$$

Species	$\Delta_{i\text{-}py}$ (at 350°C)
H_2S°	-1.03
HS^-	-1.78
S^{2-}	-4.77
all SO_4 species (mineral and aqueous)	+18.5
Pyrite	0
Chalcopyrite	-1.16

measured isotopic compositions of sulfide and sulfate minerals would be in equilibrium, as calculated from the Δ_{anh-py} value of 9.6‰ and the data of Ohmoto and Rye (1979), is nearly 620°C. This temperature is inconsistent with the temperature of vein formation determined from fluid inclusion and mineral stability data, implying that sulfur isotopic equilibrium was not established. This apparent isotopic disequilibrium between the sulfide and sulfate minerals precipitated from the mineralizing solution could have occurred for several reasons, including: 1) non-systematic isotopic disequilibrium among the various sulfur-bearing species, 2) deposition of the sulfide and sulfate minerals from different solutions of varying isotopic characters, 3) errors in the Δ values currently in use for sulfide - sulfate mineral pairs or, 4) systematic isotopic disequilibrium among the sulfur-bearing species. These possibilities will be discussed and evaluated individually below.

Non-systematic isotopic disequilibrium:

Non-systematic isotopic disequilibrium would occur in a system where the isotopic compositions of sulfur-bearing species not only failed to reach, or approach, internally consistant equilibrium values, but also deviated from the calculated equilibrium distributions in an apparently non-systematic manner. If non-systematic disequilibrium applies to the sulfur isotope system in this study, then the sulfur isotopic composition of the ore-forming fluid can not be calculated. While this possibility can not be ruled out,

the fact that sulfur isotopes have been demonstrated to behave systematically in other similar hydrothermal systems (Field and Gustafson, 1976; Ohmoto and Rye, 1979; Shelton and Rye, 1982) requires that other possible explanations be considerd.

Deposition of minerals from isotopically distinct solutions:

The apparent isotopic disequilibrium observed in this study could have arisen from the equilibrium precipitation of the sulfide and sulfate minerals from isotopically distinct solutions; either from two separate solutions using the same vein as a pathway or from the same solution at different times as the sulfur isotopic composition and/or the relative distribution of aqueous sulfur species in solution varied.

The lack of observed reaction rims or replacement textures in the vein-filling minerals is evidence that the minerals, once deposited, were never significantly out of equilibrium with vein fluids. It is unlikely that a second solution, encountering the vein-filling assemblage of an earlier solution, would be in equilibrium with all of the minerals previously deposited. Evidence for two separate solutions is also lacking at a larger scale at Sierrita. Preece and Beane (1982) report vein-filling assemblages from several locations in the biotite quartz diorite which are nearly identical to the assemblage present in this study. Field (1981), in an unrelated study, reports $\delta^{34}S$ values for chalcopyrite and anhydrite from a single vein in the biotite quartz diorite at Sierrita of -1.1‰ and

+9.7°/oo, respectively. These values are very similar to those determined in this study (-2.0°/oo and +8.8°/oo, respectively), and the $\Delta_{anh-cpy}$ values in both cases are identical (10.8°/oo), indicating the same degree of sulfur isotopic disequilibrium in each vein. For a two solution model to account for the apparent sulfur isotopic disequilibrium, it would be necessary for both solutions to have circulated extensively throughout the biotite quartz diorite along the same channel-ways. Further, as Preece and Beane (1982) have documented a minimum of five discrete mineralizing cycles, the two solution model would require a minimum of five repetitions of the two solutions, the second following the first along each vein as it formed. Such a recurrence of two distinct solutions along each vein seems improbable at best and is the major drawback of the two solution model as an explanation for the observed isotopic relationships.

Evidence for the chemical evolution of the hydrothermal solution with time is seen in the repeated 'potassic' to 'propylitic' alteration sequences reported by Preece and Beane (1982). Changes in the chemical conditions prevailing in the solution could have led to the deposition, at different times, of sulfide and sulfate minerals each of which was in isotopic equilibrium with the fluid at the time of deposition. The isotopic composition of total aqueous sulfur, and hence the isotopic composition of minerals precipitated from the solution, could change with time as sulfur-bearing minerals were deposited and/or dissolved. Alternately, changes in the physio/chemical conditions prevailing in the solution could change the

relative distribution of aqueous sulfur species in solution which, while not affecting the sulfur isotopic composition of total aqueous sulfur, would affect the isotopic compositions of the sulfide and sulfate components.

Changes in the isotopic composition of aqueous sulfur is to be expected as sulfur-bearing minerals are precipitated from, or dissolved by, the hydrothermal solution. In each of the six veins from the biotite quartz diorite studied by Preece and Beane (1982), the vein-filling mineralogy evolved from an early 'potassic' phase, characterized by alkali feldspar and biotite, to a later 'propylitic' phase, characterized by epidote, chlorite and sulfides. This mineralogic evolution was accompanied by a 25 - 50°C decrease in temperature. In five of the six veins they studied, anhydrite was deposited with the 'potassic' assemblage. However, sulfides were notably absent from this early mineralization in all veins studied. In general, $\delta^{34}S$ values for sulfate minerals at Sierrita fall in a fairly narrow range of +9 to +13°/oo (Ohmoto and Rye, 1979; this study). As the sulfur isotopic fractionation between aqueous and mineral sulfate species is negligable (Ohmoto and Rye, 1979), a value of +10°/oo may be considered representative of aqueous sulfates. The equilibrium composition of coexisting aqueous sulfides, at 350 to 400°C would have been between -5 and -10°/oo and, at the aqueous sulfide : sulfate ratio calculated in this study of 1 : 1, total aqueous sulfur would have been between 0 and +5°/oo.

Later solutions passing along the same channel ways could dissolve previously deposited anhydrite. If the sulfur isotopic compositions of the 'potassic' and 'propylitic' solutions were the same originally (0 to 5°/oo), the addition of sulfur with $\delta^{34}S = +10°/oo$ would increase the $\delta^{34}S$ value of total aqueous sulfur. Furthermore, if the ratio of aqueous sulfide to sulfate were maintained at 1 : 1 (this ratio being governed primarily by solution pH and f_{O_2}) then dissolution of enough anhydrite to yield a $\delta^{34}S$ value of total aqueous sulfur of +8 to +10°/oo would allow the subsequent equilibrium precipitation of sulfide minerals with $\delta^{34}S$ values similar to those measured in this study. In order to accomplish the required shift in the isotopic composition of total aqueous sulfur, between two and ten times the amount of sulfur originally present in the solution would have to be acquired by anhydrite dissolution.

In the vein-filling assemblage described in this study, anhydrite and the sulfides pyrite and chalcopyrite were seen to be part of the vein center assemblage. Textures indicating replacement of anhydrite by the sulfides were not noted. Neither are indications of anhydrite deposition and subsequent redissolution at Sierrita reported in the literature. Thus this mechanism does not appear to be the cause of the apparent isotopic disequilibrium.

Chemical evolution of the hydrothermal solution, and the attendant redistribution of the aqueous sulfur species could lead to the observed mineral sulfur isotopic compositions without changing the isotopic composition of total aqueous sulfur. For example, if at the

time of anhydrite deposition the $\delta^{34}S$ value of aqueous sulfate was +10°/oo, the equilibrium $\delta^{34}S$ value of aqueous sulfides would be near -10°/oo, at a temperature of roughly 350°C. If the ratio of aqueous sulfide to sulfate in this solution was 1 : 3, the isotopic composition of total aqueous sulfur would have been about +5°/oo. If, over time, the aqueous sulfur was reduced to a 3 : 1 sulfide to sulfate ratio, the $\delta^{34}S_{\Sigma S_{aq}}$ would remain unchanged, but the equilibrium $\delta^{34}S$ values of aqueous sulfides would now be near 0°/oo, and pyrite and chalcopyrite deposited from this solution would have $\delta^{34}S$ values comparable to those measured in this study.

At the pH calculated in this study (5.8), a decrease of 1/2 log f_{O_2} unit could be sufficient to change the aqueous sulfide to sulfate ratio from 1 : 3 to 3 : 1. Such a reduction would be expected in a solution moving from a relatively felsic rock (the quartz monzonite porphyry) to a more mafic one (the biotite quartz diorite). Conversely, at the f_{O_2} calculated in this study (log f_{O_2} = -27.5), a decrease of 1 pH unit could also serve to effect the required species redistribution. These effects of changes in solution chemistry can be seen graphicaly in Figure 10. The 1/2 log f_{O_2} unit shift from sulfate to sulfide dominance would, at the pH calculated in this study, require a change from the solution being hematite stable to magnetite stable. A shift from hematite to magnetite is not seen in the vein studied, nor was hematite found in more than trace amounts in other veins in the biotite quartz diorite by Preece and Beane (1982). However, the relatively minor amounts, or even absence, of

hematite does not necessarily preclude the solution having been stable with respect to hematite relative to magnetite. Reduction of such a fluid by reactions with the more mafic minerals in the biotite quartz diorite could well be the cause of sulfide deposition, while anhydrite stability was maintained by the addition of calcium from the alteration of wall rock plagioclase and hornblende discussed previously.

Changes in the isotopic composition of total aqueous sulfur due to dissolution of previously deposited sulfates does not appear to be a reasonable explanation of the apparent isotopic disequilibrium found in this study. However, chemical evolution of the solution, specific decreasing f_{O_2} or pH resulting in changes in the relative distribution of aqueous sulfur species, could have led to the observed isotopic compositions. In either case it is not possible to directly calculate the isotopic composition of total aqueous sulfur because the deposition of the sulfides and sulfates occurred at different times from changing solutions. However, both models do place constraints on total aqueous sulfur, limiting possible values to between -5 and +10‰.

Errors in the isotopic enrichment factors:

The generally accepted isotopic enrichment factors for sulfide-sulfate isotopic fractionations reported in the literature were derived from theoretical considerations (Sakai, 1968). The apparent isotopic disequilibrium found in this study could have arisen

from errors in these values. However, evaluation of such a possibility is beyond the scope of this study.

Systematic isotopic disequilibrium:

Systematic isotopic disequilibrium, or heterogeneous isotopic equilibrium is the condition where isotopic equilibrium is established among the sulfide species and among the sulfate species but not between them. Shelton and Rye (1982) suggested this as an explanation for similar apparent isotopic disequilibrium observed at the Gaspé porphyry copper deposit. Such isotopic disequilibrium would not necessarily imply chemical disequilibrium between the sulfur-bearing species, but rather that isotopic equilibration is slow relative to chemical reaction rates involving sulfides and sulfates. The isotopic compositions of aqueous sulfide and sulfate species could be inherited from earlier solution conditions and preserved meta-stably in the solution until the time of mineralization in the studied vein. For example, at 'magmatic' temperatures of roughly 700°C, the equilibrium $\Delta_{\text{sulfate-sulfide}}$ value is +4 to +5‰ (Ohmoto and Rye, 1979). If, after establishing the isotopic compositions of species at such a temperature, the fluid was cooled rapidly, relative to the time required for sulfide-sulfate isotopic equilibration such that sulfur isotopic equilibrium was not reached, the resulting $\delta^{34}S$ values of minerals precipitated from the solution might exhibit $\Delta_{\text{sulfate-sulfide}}$ values similar to those measured here. Other possible mechanisms resulting in a systematic isotopic disequilibrium include: relatively

rapid mixing of sulfide- and sulfate- rich fluids, local dissolution of sulfur-bearing minerals, or relatively rapid changes in solution chemistry.

Regardless of the cause, or causes, of the isotopic disequilibrium between the aqueous sulfides and sulfates, if the departure from equilibrium is systematic with a heterogeneous isotopic equilibrium established among the sulfides and sulfates independently, then calculation of the isotopic composition of total aqueous sulfur can be accomplished by considering sulfides and sulfates separately. Isotopic equilibrium among the sulfates implies that the +8.8°/oo $\delta^{34}S$ value measured for anhydrite is representative of all aqueous sulfates (Ohmoto and Rye, 1979). The $\delta^{34}S$ values of aqueous sulfides can be calculated from the isotopic composition of pyrite and the isotopic enrichment factors listed in Table 9. The isotopic compositions of the various sulfur species calculated under the assumption of a systematic disequilibrium are listed in Table 8. Employing these values along with the molar distribution of aqueous sulfur species previously calculated in Equation 5 yields an isotopic composition of total aqueous sulfur of +3.5°/oo.

Discussion

If the isotopic disequilibrium is a result of non-systematic sulfur isotopic fractionations, or the result of depositions of the vein-filling minerals from two or more different solutions, then the calculation of isotopic composition of total aqueous sulfur is not

possible. This possibility can not be overlooked. However, similar apparent sulfur isotopic disequilibrium behavior has been shown to be systematic in its departure from equilibrium in two other porphyry copper systems. For the Gaspé porphyry copper deposit in Quebec, Canada and the El Salvador porphyry copper deposit in Chile, Shelton and Rye (1982) have suggested that the sulfur isotopic data imply a systematic disequilibrium or heterogeneous equilibrium, where sulfur isotopic equilibrium existed among the sulfide species and among the sulfate species, but not between the two sets of species. If this concept is applied to the Sierrita porphyry copper deposit, then the isotopic compositions of aqueous sulfide and sulfate species can be calculated independently from the measured isotopic compositions of sulfide and sulfate minerals precipitated from the solution. The sulfur isotopic composition of total aqueous sulfur in the hydrothermal solution responsible for mineralization calculated under the assumption of systematic isotopic disequilibrium is $\delta^{34}S_{\Sigma S_{aq}}$ = +3.5°/oo.

The significance of this calculated isotopic composition of aqueous sulfur is illustrated in Figure 10, a summary of the characteristic sulfur isotopic signatures of generalized sulfur sources. Sulfides of igneous origin generally have $\delta^{34}S$ values near 0 °/oo(± 5°/oo). Sedimentary sulfides (commonly biogenic) have a very large range of values, but are usually isotopically light, having large negative $\delta^{34}S$ values. Sedimentary sulfates (evaporites) generally have positive $\delta^{34}S$ values between +10 and +30°/oo. The line

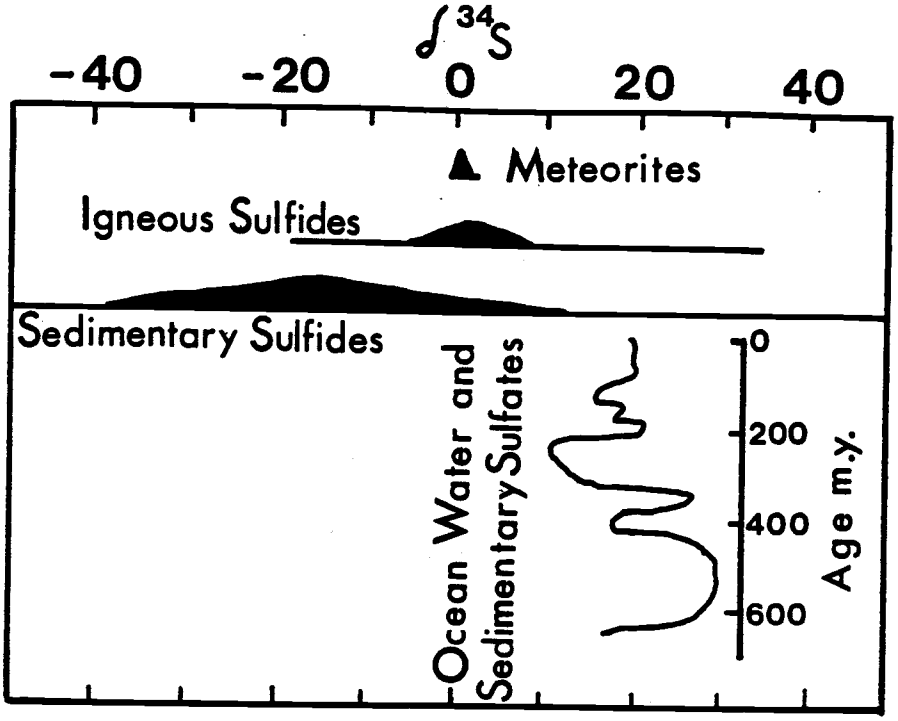

Figure 10. ^{34}S values typical of various generalized sulfur resevoirs.

The insert indicates the changes in the sulfur isotopic composition of marine evaporite sulfates with time in the Phanerozoic. 0% is defined as the sulfur isotopic composition of the mineral troilite from the Canon Diable meteorite. From Ohmoto and Rye, 1979.

in the insert in Figure 10 shows the variation in $\delta^{34}S$ values of marine evaporite sulfur through the Phanerozoic. The $\delta^{34}S_{\Sigma S_{aq}}$ = + 3.5°/oo calculated above indicates a probable igneous source for the aqueous sulfur. It is important to note here that an indicated igneous source does not necessarily imply a 'magmatic' origin for the sulfur, because no distinction is, or can be, made between sulfur evolved from a cooling or crystalizing magma (a syn-mineralization intrusive) and sulfur leached from pre-mineralization intrusive rocks by circulating hydrothermal fluids.

When calculated, or measured, sulfur isotopic compositions of aqueous sulfur are used to determine the source of sulfur in hydrothermal fluids, it is implied that the composition calculated for the mineralizing solution accurately represents the original isotopic composition of the hydrothermal fluid upon obtaining its sulfur. However, the fluid depositing the minerals seen in the vein studied here has an uncertain and potentially complex history between the time the solution acquired its sulfur and the time of deposition of the minerals in the vein studied. The precipitation of minerals from the solution prior to deposition at this vein could have changed the isotopic composition of the fluid by selectively removing relatively heavy, or light, sulfur from the fluid into the mineral phases. Since the ultimate source of the sulfur is best represented by the isotopic composition of the fluid prior to deposition of any sulfur-bearing minerals, it is necessary to modify Equation 5 in order to account for this previously precipitated sulfur:

$$\delta^{34}S_{original} = \frac{(\delta^{34}S_{\Sigma S_{aq}} \cdot m_{\Sigma S_{aq}}) + \sum_j (\delta^{34}S_j \cdot m_j)}{(m_{\Sigma S_{aq}} + \sum_j m_j)} \qquad (65)$$

In this equation, '$\delta^{34}S_j$' and 'm_j' are the isotopic composition and number of moles per 1000 g of H_2O, respectively, of sulfur precipitated as mineral phase(s) 'j' prior to the arrival of the solution at the point in the system represented by the studied vein.

To relate the $\delta^{34}S_{\Sigma S_{aq}}$ value calculated in this paper to that of the original hydrothermal fluid requires knowledge of the identity and number of moles of the sulfur-bearing minerals which have precipitated from (and/or been dissolved by) the solution along its path to the point at which the sample was collected for study. It is beyond the scope of this study to attempt a rigorous determination of these parameters. However, the effects of previous depositions can be evaluated qualitatively. Immediately prior to arrival at the studied vein, a sulfate mineral precipitated from the solution would have a $\delta^{34}S$ value of near 9°/oo, which is 5°/oo heavier than the solution from which it precipitated. This means that the $\delta^{34}S$ of the solution immediately prior to deposition of this sulfate was greater than it was afterwards. Conversely, a sulfide mineral deposited immediately prior to arrival at the studied vein would have a $\delta^{34}S$ value on the order of -2°/oo, indicating an isotopically lighter original solution.

Estimates of the amounts of sulfide and sulfate minerals deposited from the solution can be made. If, for example, it is

assumed that the mineralogy of the studied vein is representative of minerals previously precipitated from the fluid, then the predominance of sulfides over anhydrite (visually estimated to be 5 : 1) in the hand sample would indicate a lower original $\delta^{34}S$ of solution than that calculated here. However, a comparison of fluid inclusion data and mineralogy of the studied vein with those of Preece and Beane's BQD - 02 vein (Table 3) indicates that the vein studied here corresponds to the later 'propylitic' portion of a mineralizing cycle. In each of the cycles documented by Preece and Beane (1982), deposition of a 'potassic' assemblage, often containing anhydrite but not sulfides, preceded the 'propylitic' phase which commonly contained both anhydrite and sulfides. If it is assumed that the solution responsible for mineralization in the studied vein had a history similar to those documented by Preece and Beane, then a significant amount of anhydrite might have been deposited elsewhere in the 'potassic' assemblage and not be represented in the vein assemblage seen in this study. For example, if the original solution had deposited an amount of anhydrite equivalent to the amount of sulfur determined to have been present when formation of the vein occurred (i.e., the original solution contained twice as much dissolved sulfur as the solution forming the vein studied), then the solutions original $\delta^{34}S$ value would have been approximately $+7^{o}/oo$. In order to shift the sulfur isotopic composition of the solution to an original value compatible with a sedimentary sulfate source of the aqueous sulfur (i.e. to $+10^{o}/oo$) it would be necessary for the original fluid to have

contained nearly ten times the 0.004 molal concentration of sulfur calculated for the mineralizing solution in this study and 90% of that original sulfur would have to have been precipitated as anhydrite. Such large amounts of anhydrite, relative to the amounts of sulfide present at Sierrita, have not been found. Thus prior deposition can not be invoked to account for the relatively light $\delta^{34}S$ of the solution if the sulfur was originally from a sedimentary source. However, some contribution from such a sulfate source to the total sulfur content of the solution can not be ruled out.

The establishment of equilibrium is an assumption which is behind the chemical and isotopic calculations made in this study, yet the measured $\delta^{34}S$ values of the sulfide and sulfate minerals present in the vein indicate a system which is not completely in equilibrium. The preceding discussions of potential causes of sulfur isotopic disequilibrium all assumed a system in which vein-filling minerals and the hydrothermal solution were in chemical equilibrium. And yet, the deposition of the minerals may well have been the product of a solution, out of equilibrium with its surroundings, attempting to move towards equilibrium. If chemical equilibrium was not reached, or at least closely approximated, then not only must the behavior of the isotopes in sulfur-bearing species be questioned, but the calculated distribution of aqueous sulfur species must also be suspect. Ohmoto and Lasaga (1982), in their study on aqueous sulfide and sulfate kinetics, suggest that for a cooling hydrothermal fluid in a fracture controlled system at temperatures below about 350°C, the attainment of

sulfide-sulfate equilibrium is not to be expected. Minerals deposited from a solution out of equilibrium with its surroundings may lock into their compositions signatures of a chemical environment intermediate to those which might best describe the solution and the surroundings. Further, the 'assemblage' of minerals precipitated under such conditions may be the result of various segments of the solutions' chemistry attempting to equilibrate with their surroundings rather than the solution as a whole depositing an 'equilibrium assemblage', strictly defined.

Because of the uncertainties in both the sulfur isotopic and chemical behavior of a system not at, or near, equilibrium, the isotopic composition of total aqueous sulfur can not be calculated with any degree of confidence under such conditions. However, some constraints can be placed on the nature of aqueous sulfur at Sierrita. Since the sulfur isotopic fractionation is negligible among sulfate species, both aqueous and mineral, the isotopic composition of anhydrite is a measure of the composition of the aqueous sulfates. The narrow range in $\delta^{34}S$ values of sulfate minerals (anhydrite and gypsum) determined at Sierrita (+9 to +13‰) indicates a $\delta^{34}S$ value consistant with a marine evaporite, specifically one of Permian age, as the source of aqueous sulfates. Similarly, Shelton and Rye (1982) demonstrated that aqueous and mineral sulfides may establish equilibrium relatively quickly in porphyry copper deposits. If this is the case at Sierrita, then the measured isotopic compositions of the pyrite and chalcopyrite imply that the sulfide fraction of total

aqueous sulfur had an isotopic composition between -5 and 0‰, a range most consistent with an igneous sulfur source. The relative importance of these two potential sulfur sources is proportional to their relative molalities in solution, which in turn is governed by solution chemistry and the degree of equilibrium established in the system.

SUMMARY AND CONCLUSIONS

When applying sulfur isotopy to problems in the origins of mineralization in porphyry copper systems it is necessary to determine the sulfur isotopic composition of the hydrothermal solution from which the ores formed. In a system at equilibrium, the $\delta^{34}S$ value of aqueous sulfur can be calculated from a knowledge of the physio-chemical parameters governing the distribution of aqueous sulfur species (temperature, pressure, ionic strength, oxygen fugacity, pH and the activities of the Na^+, K^+ and Ca^{2+} ions in the solution) combined with the isotopic composition of a sulfur-bearing mineral precipitated from the solution. In order to minimize problems arising from spatial and temporal variations in solution conditions within the system, these parameters were determined from a single vein from the Sierrita porphyry copper deposit. Based on the assumption of solution - mineral equilibrium the following information was obtained:

1) From fluid inclusion analysis of vein quartz the temperature, pressure and ionic strength (salinity) of the solution were found to be 350°C, 330 bars and 1.14 molal NaCl equivalent, respectively.

2) From equilibrium mineral stability and composition data the following were caluclated; $\log f_{O_2} = -27.5$, pH = 5.8, $a_{Na^+} = 6.3 \times 10^{-2}$, $a_{K^+} = 9.8 \times 10^{-3}$, and $a_{Ca^{2+}} = 1.0 \times 10^{-5}$.

From these data the relative molar distribution of aqueous sulfur species is calculated to be; H_2S^o = 49.5%, HS^- = 0.6%, SO_4^{2-}= 10.8%, HSO_4^- = 37.4% and KSO_4^- = 1.7%. Other species, while present, are not significant under these conditions.

The measurement of $\delta^{34}S$ values of apparently coexisting sulfide (pyrite = -0.8°/oo, chalcopyrite = -2.0°/oo) and sulfate (anhydrite = +8.8°/oo) minerals are not compatable with isotopic equilibrium at, or near, 350°C, the sulfur isotopic temperature of formation indicated by these measurements being 620°C. These disequilibrium $\delta^{34}S$ values for the vein-filling minerals bring into question the assumption of equilibrium behind all the chemical and isotopic calculations made in this study, making any determination of the sulfur isotopic composition of aqueous sulfur questionable.

However, assuming that chemical equilibrum was at least approached, as suggested by the petrographic relationships observed among the vein-filling minerals and the similarity of the results of this study with those reported from other porphyry copper deposits, and assuming heterogeneous isotopic equilibrium among the sulfur-bearing species, based on the relatively slow sulfur isotopic equilibration of sulfide and sulfate species, the isotopic composition of total aqueous sulfur is calculated to be +3.5°/oo. This value is most compatible with an igneous sulfide source for the sulfur. Consideration of the two disequilibrium sulfur populations, sulfides and sulfates, separately tends to indicate a dual sulfur source. The

$\delta^{34}S$ values of aqueous sulfide (-5 to 0‰) implying an igneous sulfur source while the $\delta^{34}S$ values of sulfates (≈ + 10‰) is best explained by a (Permian) sedimentary sulfate sulfur source.

APPENDIX A

SEMQ Analyses:

Compositions of minerals used in this study were determined at the University of Arizona, Department of Planetary Sciences, on an ARL Scanning Electron Microprobe Quantometer (SEMQ) together with a Tracor-Northern system for the reduction of data. Internal laboratory standards whose compositions are accurately known were used to calibrate the system. Elements analyzed for in the feldspars and epidotes were: Na, K, Ca, Al, Si, Mg, Mn, Fe and Ti. The results are expressed as weight percent oxides. The SEMQ is not capable of distinguishing between Fe^{2+} and Fe^{3+} in its analyses, so total iron has been assumed to be in the ferric state and given as Fe_2O_3.

The results have been recalculated into mineral compositions based on the number of oxygens in the ideal mineral formula. Since structural water can not be measured on the SEMQ, it has been deleted from the mineral composition calculations of the epidotes. For the feldspars, the mineral composition was based on eight oxygens, epidote compositions are based on twelve and one half oxygens.

Analyses of the fused sulfide powder were for the elements Cu, Fe and S. Qualitative analyses indicated that only trace amounts of other base metals were present. Results from these analyses are given in weight percent of each element in the sample.

Appendix A
Table 1. SEMQ Analyses of Feldspars

Oxide Weight Percent

	1	2	3	4	5	6	7	8	9
Na_2O	5.93	7.41	7.35	8.56	8.89	5.82	6.42	7.28	6.90
K_2O	0.11	0.18	2.75	0.13	0.13	0.55	0.14	0.16	0.16
CaO	9.64	6.56	1.74	2.07	2.39	7.80	8.10	6.55	6.94
SiO_2	54.69	58.64	59.01	65.43	61.87	52.22	55.68	57.48	57.56
Al_2O_3	27.34	24.88	24.38	18.80	22.68	27.13	26.33	25.07	25.43
Fe_2O_3	0.22	0.25	0.19	0.08	0.17	0.25	0.08	0.07	0.12
Totals	97.93	97.92	95.42	95.07	96.99	93.77	96.75	96.61	97.11

Molecular Formula Based on 8 Oxygens

Na	0.53	0.65	0.66	0.76	0.78	0.54	0.58	0.65	0.61
K	0.01	0.01	0.16	0.01	0.06	0.03	0.01	0.01	0.01
Ca	0.47	0.32	0.09	0.10	0.12	0.40	0.40	0.32	0.34
Si	2.51	2.67	2.74	2.99	2.81	2.50	2.57	2.65	2.64
Al	1.48	1.33	1.33	1.01	1.22	1.53	1.43	1.36	1.37
Fe(III)	0.01	0.01	0.01	---	0.01	0.01	---	---	---

Appendix A
Table 1. SEMQ Analyses of Feldspars - continued

Oxide Weight Percent

	10	11	12	13	14	15
Na_2O	0.07	8.87	7.51	9.22	1.85	9.75
K_2O	0.02	0.95	0.83	0.15	13.44	1.05
CaO	20.11	6.98	7.37	0.95	0.14	2.04
SiO_2	42.49	58.38	58.29	69.25	62.75	61.79
Al_2O_3	34.29	21.23	23.75	17.56	19.63	22.30
Fe_2O_3	---	0.40	0.69	0.04	0.29	0.12
Totals	96.98	96.91	98.44	97.17	98.10	97.05

Molecular Formula Based on 8 Oxygens

Na	0.01	0.80	0.66	0.80	0.17	0.86
K	---	0.06	0.05	0.01	0.80	0.06
Ca	1.03	0.36	0.36	0.05	0.01	0.10
Si	2.03	2.72	2.66	3.08	2.93	2.82
Al	1.93	1.47	1.28	0.92	1.08	1.20
Fe(III)	---	0.01	0.02	---	0.01	---

Appendix A

Table 2. SEMQ Analyses of Epidotes

Oxide Weight Percent

	1	2	3	4	5	6	7	8
Na_2O	0.02	0.07	---	0.03	---	0.02	0.02	---
K_2O	0.01	0.01	---	---	---	---	0.01	---
CaO	22.05	22.08	22.07	22.56	17.44	25.71	22.37	22.68
Al_2O_3	21.99	22.36	19.80	19.69	15.46	19.89	19.80	22.95
Fe_2O_3	15.21	15.31	18.79	18.26	12.82	13.19	18.47	14.35
MnO	0.31	0.30	0.09	0.01	0.13	0.39	0.10	0.16
TiO_2	---	0.06	---	0.01	0.04	0.05	---	0.06
SiO_2	37.07	37.74	36.65	36.83	52.69	32.38	36.51	36.94
Totals	96.66	97.93	97.40	97.39	98.58	91.63	97.28	97.14
Molecular Formula Based on 12.5 Oxygens								
Na	---	0.01	---	---	---	---	---	---
K	---	---	---	---	---	---	---	---
Ca	1.99	1.96	2.02	2.06	1.41	2.41	1.96	1.96
Al	2.19	2.19	2.00	1.98	1.38	2.05	1.91	2.18
Fe(III)	0.97	0.96	1.21	1.18	0.73	0.86	1.14	0.86
Mn	0.02	0.02	0.01	---	0.01	0.03	0.01	0.01
Ti	---	---	---	---	---	---	---	---
Si	3.31	3.14	3.14	3.15	3.97	2.83	2.98	2.98
Fe/Fe+Al	0.92	0.91	1.13	1.12	1.04	0.89	1.12	0.85

Appendix A

Table 2. SEMQ Analyses of Epidotes - continued

Oxide Weight Percent

	9	10	11	12	13	14	15	16
Na_2O	0.06	0.01	0.03	----	0.01	-----	0.02	0.03
K_2O	-----	0.01	---	0.01	0.02	0.02	0.01	---
CaO	22.63	21.40	22.41	22.34	22.55	21.92	22.31	22.30
Al_2O_3	21.65	22.05	19.24	21.73	21.54	20.50	21.91	21.49
Fe_2O_3	15.96	15.11	19.32	15.44	15.51	17.00	15.24	15.84
MnO	0.09	0.73	0.09	0.17	0.12	0.06	0.08	0.17
TiO_2	0.05	0.06	---	0.03	0.06	---	0.02	0.05
SiO_2	37.06	35.61	36.16	36.07	36.12	36.38	36.57	36.22
Totals	97.50	94.98	97.25	95.79	95.91	95.88	96.16	96.10
Molecular Formula Based on 12.5 Oxygens								
Na	0.01	---	---	---	---	---	---	---
K	---	---	---	---	---	---	---	---
Ca	1.96	1.90	1.97	1.97	1.98	1.94	1.95	1.96
Al	2.06	2.16	1.86	2.10	2.08	1.99	2.11	2.07
Fe	0.97	0.94	1.20	0.96	0.96	1.05	0.94	0.98
Mn	0.01	0.05	0.01	0.01	0.01	---	0.01	0.01
Ti	---	---	---	---	---	---	---	---
Si	2.99	2.95	2.97	2.97	2.97	3.00	2.99	2.97
Fe/Fe+Al	0.96	0.91	1.17	0.94	0.95	1.04	0.92	0.96

Appendix A

Table 2. SEMQ Analyses of Epidotes - continued

Oxide Weight Percent

	17	18	19	20	21	22	23	24
Na_2O	---	0.01	0.12	0.02	---	---	0.01	0.02
K_2O	0.02	0.07	0.04	0.03	0.03	0.03	0.03	0.04
CaO	22.30	21.74	21.58	22.43	21.70	21.85	21.17	19.75
Al_2O_3	18.36	18.50	18.64	20.95	16.55	17.60	16.97	13.93
Fe_2O_3	17.70	16.61	15.88	13.70	16.92	14.97	15.38	15.91
MnO	---	0.18	0.25	0.07	0.08	0.43	0.04	0.08
TiO_2	---	---	---	0.01	---	0.05	---	0.02
SiO_2	36.87	36.94	36.98	37.18	36.72	36.81	36.30	43.17
Totals	95.29	94.05	93.49	94.39	92.00	91.74	91.26	92.92
Molecular Formula Based on 12.5 Oxygens								
Na	---	---	0.02	---	---	---	---	---
K	---	0.01	---	---	---	---	---	---
Ca	1.91	1.88	1.87	1.91	1.92	2.01	1.98	1.77
Al	1.73	1.76	1.78	1.96	1.61	1.78	1.75	1.37
Fe	1.06	1.01	0.97	0.82	1.05	0.97	1.00	1.00
Mn	---	0.01	0.02	---	0.01	0.03	0.01	0.01
Ti	---	---	---	---	---	---	---	---
Si	2.95	2.98	2.99	2.95	3.04	3.16	3.17	3.59
Fe/Fe+Al	1.14	1.09	1.06	0.88	1.18	1.06	1.10	1.27

Appendix A

Table 2. SEMQ Analyses of Epidotes - continued

Oxide Weight Percent

	25	26
Na_2O	0.04	0.07
K_2O	0.02	---
CaO	22.57	22.87
Al_2O_3	22.89	21.97
Fe_2O_3	14.58	15.52
MnO	0.10	0.22
TiO_2	0.05	0.39
SiO_2	36.75	37.84
Totals	97.00	98.88
Molecular Formula Based on 12.5 Oxygens		
Na	0.01	0.01
K	---	---
Ca	1.95	1.95
Al	2.18	2.04
Fe	0.89	0.93
Mn	0.01	0.02
Ti	---	0.02
Si	2.97	3.01
Fe/Fe+Al	0.87	0.94

Appendix A

Table 3. SEMQ Analyses of the Fused Sulfide Powder

	Weight Percent			Mole Fraction
	Cu	Fe	S	Cu / Fe + Cu
1	21.6	45.9	32.4	0.29
2	21.0	46.3	32.7	0.28
3	23.8	45.1	31.1	0.32
4	23.0	47.3	30.0	0.30
5	21.0	46.6	32.4	0.28
6	20.0	47.4	32.5	0.27
7	28.0	38.4	33.6	0.38
8	27.7	38.8	33.5	0.38
9	22.1	47.5	30.3	0.29
10	20.2	47.1	32.7	0.27
11	22.5	44.1	33.3	0.31
12	20.5	46.6	32.8	0.28
13	21.1	48.4	30.5	0.27
14	28.4	40.3	31.3	0.37
15	22.6	49.0	31.2	0.29
16	20.4	46.8	37.8	0.30
			Average	0.305

LIST OF SYMBOLS AND ABBREVIATIONS

Symbol	Explanation
$\delta^{34}S_i$	Sulfur isotopic composition of species 'i'
Δ_{a-b}	Sulfur isotopic enrichment factor
α_{a-b}	Sulfur isotopic fractionation factor
ΣS_{aq}	Total aqueous sulfur
X_i	Mole fraction represented by species 'i'
m_i	Molality of species 'i' in solution
a_i	Activity of species 'i' in solution
K_i	Equilibrium reaction constant for reaction 'i'
f_{O_2}	Fugacity of oxygen
γ_i	Individual ion activity coefficient
$\mathring{\gamma}_i$	Stoichiometric ion activity coefficient
T_H	Fluid inclusion homogenization temperature

Abbreviation	Mineral
Ab	Sodium Feldspar
An	Calcium Feldspar
anh	Anhydrite
bio	Biotite
chl	Chlorite
clino	Clinozoisite
cpy	Chalcopyrite
epid	Epidote
gr	Grossular Garnet
hem	Hematite
mgt	Magnetite
mo	Molybdenite
Or	Potassium Feldspar
py	Pyrite
qtz	Quartz
ser	Sericite (Muscovite)

LIST OF REFERENCES

Aiken, D. M., and West, R. J., 1978, Some geologic aspects of the Sierrita-Esperanza copper-molybdenite deposit, Pima County, Arizona; Ariz. Geol. Soc. Digest, vol. 11, p. 117-128.

Ault, W. V., and Jensen, M. L., 1963, Summary of sulfur isotope standards, in Biogeochemistry of Sulfur Isotopes, Jensen, M. L. (ed.), Natl. Sci. Found. Proc., Yale Univ., April 12-14, 1962, p. 16-29.

Banks, N. G., 1980, Sulfur and copper in magmas and rocks, in Advances in Geology of the Porphyry Copper Deposits, Southwestern North America, Titley, S. R. (ed.), Univ. of Ariz. Press, Tucson, 560 p.

Bird, D. K., and Helgeson, H. E., 1980, Chemical interaction of aqueous solutions with epidote-feldspar mineral assemblages in geologic systems, I, Thermodynamic analysis of phase relations in the system $CaO-FeO-Fe_2O_3-Al_2O_3-SiO_2-H_2O-CO_2$: Am. Jour. Sci., vol. 280, p. 907-941.

Bird, D. K, 1982, personal communication, research associate, Department of Geosciences, University of Arizona, Tucson.

Chaffee, M. A., 1982, A geochemical study of the Kalamazoo porphyry copper deposit, in Advances in Geology of the Porphyry Copper Deposits, Titley, S. R. (ed), Univ. of Ariz. Press, Tucson, 560p.

Cooper, J. R., 1973, Geologic map of the Twin Buttes quadrangle, southwest of Tucson, Arizona: U. S. Geol. Surv. Misc. Geol. Inv., Map I-745.

Denis, M., 1974, Alterations et fluides associes dans le porphyre cuprifere de Serrits: Unpublished Disertation, 3° Cycle, University of Nancy, France, 149 p.

Faure, G., 1977, Principles of Isotope Geochemistry, John Wiley and Sons, Inc., New York, 464 p.

Fellows, M. L., 1976, Composition of epidote in porphyry copper deposits: Unpublished Masters Thesis, Univ. of Arizona., Tucson, 190 p.

Field, C. W. and Gustafson, L. B., 1976, Sulfur Isotopes in the porphyry copper deposit at El Salvador, Chile: Econ. Geol., v. 71, p. 1533-1548.

References--continued

Field, C. W., 1981, personal communication, Professor, Department of Geology, Oregon State University, Corvallis.

Garrells, R. M., and Christ, C. L., 1965, Solutions, Minerals and Equilibria: Freeman, Cooper and Co., San Francisco, 450p.

Haynes, F. M., 1980, The evolution of fracture-related permiability within the Ruby Star granodiorite, Sierrita porphyry copper deposit, Pima County, Arizona: Econ. Geol. vol. 75, p. 673 - .

Helgeson, H. C., 1969, Thermodynamics of hydrothermal systems at elevated temperatures and pressures: Am. Jour. Sci., vol. 267, p. 729-804.

_____, and Kirkham, D. H., 1974, Theoretical prediction of the thermodynamic behavior of aqueous electrolytes at high pressures and temperatures; Parts I and II: Am. Jour. Sci., vol. 274, p. 1089-1261.

_____, Delany, J. M., Nesbitt, H. W., and Bird, D. K., 1978, Summary and critique of the thermodynamic properties of rock-forming minerals: Am. Jour. Sci., vol. 278-A, p. 1-229.

Lynch, D. W., 1966, The economic geology of the Esperanza mine and vicinity, in Geology of the Porphyry Copper Deposits, Titley, S. R., and Hicks, C. L. (eds.), Univ. of Ariz. Press, Tucson, p. 267-279.

Nash, J. T., 1975, Fluid-inclusion petrology - data from porphyry copper deposits and applications to exploration: U. S. Geol. Surv. Prof. Paper 907-D, 16p.

Ohmoto, H., 1972, Systematics of sulfur and carbon isotopes in hydrothermal ore deposits: Econ. Geol. vol. 67, p. 551-579.

_____, and Rye, R. O., 1979, Isotopes of sulfur and carbon, in Geochemistry of Hydrothermal Ore Deposits, second edition, Barnes, H. L. (ed.), John Wiley and Sons, Inc., New York, p. 509-567.

_____, and Lasaga, A. C., 1982, Kinetics of reactions between aqueous sulfates and sulfides in hydrothermal systems: Geoch. and Cosomoch. Acta, v. 46, p. 1727.

Parsons, I., 1978, Alkali-feldspars: which solvus?, in Physics and Chemistry of Minerals, vol. 2, p. 199-213.

References--continued

Potter, R. W., Jr., 1977, Pressure corrections for fluid-inclusion homogenization temperatures based on volumetric properties of the system NaCl-H_2O: U. S. Geol. Surv. Journ. Res., vol. 5, no. 5, p. 603-607.

_____, Clynne, M. A., and Brown, D. L., 1978, Freezing point depression of aqueous sodium chloride solutions: Econ. Geol., vol. 73, p. 284-285.

Preece, R. K., III, 1979, Paragenesis, geochemistry and temperatures of formation of alteration assemblages at the Sierrita deposit, Pima County, Arizona: Unpublished Masters Thesis, Univ. of Ariz., Tucson, 106 p.

_____, Beane, R. E., 1982, Contrasting evolutions of hydrothermal alteration in quartz monzonite and quartz diorite wall rocks at the Sierrita Porphyry Copper Deposit, Arizona: Econ. Geol., v. 77, p. 1621-1641.

Roedder, E., 1972, Composition of fluid inclusions: U. S. Geol. Surv. Prof. Paper 440-JJ, 164 p.

_____, 1979, Fluid inclusions as samples of ore fluids, in Geochemistry of Hydrothermal Ore Deposits, second edition, Barnes, H. L. (ed.), John Wiley and Sons, Inc., New York, p. 648-737.

Rye, R. O., and Ohmoto, H., 1974, Sulfur and carbon isotopes and ore genesis; a review: Econ Geol., vol. 69, -. 826-842.

Sakai, H., 1968, Isotopic properties of sulfur compounds in hydrothermal processes: Geochem. Jour., vol. 2, p. 29-49.

Saxena, S. K., 1973, Thermodynamics of Rock-Forming Crystalline Solutions; Springer-Verlag, New York, 188 p.

Shelton, K. L., and Rye, D. M., 1982, Sulfur isotopic compositions of ores from Mines Gaspe, Quebec: an example of sulfate-sulfide isotopic disequilibria in ore-forming fluids with applications to other porphyry-type deposits: Econ. Geol., v. 77, p. 1688-1709.

Smith, V L., 1975, Hypogene alteration at the Esperanza Mine, Pima county, Arizona: Unpublished Masters Thesis, Univ. Of Ariz., Tucson, 161 p.

References--continued

Thompson, R. C., 1981, The development of fractures in the mesozoic volcanic rocks adjacent to the Sierrita porphyry copper deposit, Pima County, Arizona: Unpublished Masters Thesis, Univ. of Ariz., Tucson, 85 p.

Turekian, K. K., 1972, Chemistry of the Earth, Holt Rinehart and Winston, Inc., 131 p.

Waldbaum, D. R., and Thompson, J. B., Jr., 1969, Mixing properties of sanadine crystalline solutions; IV, phase diagrams from equations of state: Am. Mineralogist, vol. 54, p. 1274-1298.

West, R. J., and Aiken, D. M., 1982, Geology of the Sierrita-Esperanza deposit, Pima Mining District, Pima County, Arizona, in Advances in Geology of the Porphyry Copper Deposits, Southwestern North America, Titley, S. R. (ed.), Univ. of Ariz. Press, Tucson, 560 p.